ORIGINAL ARTICLE

Elena A. Ivanova · **Luis Eduardo Jatar Montaño**

A new approach to solving the solid mechanics problems with matter supply

Abstract We discuss some aspects of using the spatial description and the finite volume method as applied to the solid mechanics problems. The main objective is to study the differential equation relating the strain measure to the velocity gradient. We show that this equation can be reduced to an integral form and the obtained equation has the structure of the balance equation without a source term. On the one hand, such form of equation for the strain measure is convenient when dynamical problems of solid mechanics are solved by using the finite volume method. On the other hand, the balance equation allows us to look at the strain measure as a parameter of state in a broader sense, not as the purely geometrical characteristic. We believe that this interpretation of the strain measure may open up new prospects for describing the processes connected with the substance supply into solids. In order to solve such problems, we suggest to add a source term into the balance equation for the strain measure. We discuss this idea from different points of view. We also solve some problems where the stress–strain state of solids is caused by the source terms in the balance equation for the strain measure.

Keywords Solid mechanics · Open systems · Strain measure · Spatial description · Eulerian description · Finite volume method · Solid front tracking

1 Introduction

There are two basic approaches to describe the kinematics of continua: the material (Lagrangian) description [1–3] and the spatial (Eulerian) description [4–6]. Moreover, there are various hybrid descriptions, see, e.g., [7–12]. The material description is usually employed to simulate the behavior of solids. We note that one can introduce several different strain measures in the material description [13]. All of them have the clear geometrical meaning, since they somehow or other characterize changes of the form and volume of the elementary part of material fixed in the reference configuration. The partial differential equations formulated via

E. A. Ivanova (✉) · L. E. J. Montaño
Higher School of Theoretical Mechanics, Peter the Great St.Petersburg Polytechnic University, Polytechnicheskaya, 29, Saint-Petersburg, Russia 195251
E-mail: elenaivanova239@gmail.com

L. E. Jatar Montaño
E-mail: luiseduardojatar22@gmail.com

E. A. Ivanova
Institute for Problems in Mechanical Engineering of Russian Academy of Sciences, Bolshoy pr. V.O., 61, Saint-Petersburg 199178, Russia

the material description can be discretized by the Finite Element Method (the FEM), see [14–16]. Recognizing all the advantages of the material description and the FEM, we do note that they have some limitations. For example, finite elements tend to significantly distort at large strains, and as a result of this, the calculation accuracy reduces. That is why, the computationally expensive remeshing techniques are often employed for large strains. Furthermore, the use of the material description and the FEM is problematic when modeling fracture processes and plastic flow of materials. Certainly, there are computational techniques allowing to overcome the difficulties associated with the material discontinuity, but they considerably complicate the numerical procedures. In addition, it takes some ingenuity to apply the material description and FEM to model the processes associated with the mass supply, such as the chemical reactions and the growth of biological tissues. Certainly, there are a number of works, which solve such problems within the framework of the material description, see, e.g., [17,18]. At the same time, the need to get over the difficulties and limitations arising from the use of the material description has been resulted in that the spatial description begins to be used in solid mechanics [19–24]. We note that, in the recent years, the spatial description is developed not only for the classical continuum, but also for the Cosserat continuum [25–32] and the Cosserat continuum with microstructure [28,33–36].

The spatial description consists in the observation of material flow through a control volume that is fixed in the reference frame or moves relative to the reference frame in a given way. Such an approach does not require the material to be continuous. That is why the spatial description is less restrictive regarding the simulated processes and has a broader range of applicability than the material one. The spatial description is usually employed for simulating the gas and fluid dynamics, the dynamics of porous materials and multi-component media, as well as the sedimentation processes and the chemical reactions. We emphasize that for a long time the spatial description was applied exclusively for gases and fluids, i.e., when the elastic part of the stress tensor is completely determined by pressure. The constitutive equations for the elastic pressure can be written in terms of the density of mass. Therefore, we do not need the strain measures in the gas and fluid dynamics. The situation is completely different in solid mechanics, where the constitutive equations for the elastic part of the stress tensor are formulated in terms of the strain measures. From a mathematical point of view, the strain measures in the spatial description seem to be exactly the same as the corresponding strain measures in the material description. However, there are several important differences. First of all, in contrast to the material description which implies two position vectors and two gradient operators, in the case of the spatial description we deal with only one position vector and only one gradient operator. Therefore, not all the strain measures that are employed in the material description have analogies among the strain measures that can be introduced in the spatial description. The second distinction between the strain measures in the material and spatial descriptions results from the fact that, in the spatial description, we cannot define the displacement vector as the difference of the current and reference position vectors, as it is done in the material description. This is due to the fact that the spatial description does not implies the reference position vector at all. Thus, using the spatial description we are forced to introduce the displacement vector as the solution of the partial differential equation relating it to the velocity vector, see, e.g., [28,29]. The displacement vector obtained in such a manner is a formally introduced characteristic. In some cases, it does not correspond to an actual displacement of some part of the material. As a result, the strain measures defined by the gradient of the displacement vector, lose the clear geometrical meaning that the strain measures have on the case of the material description. The third distinction is connected with the fact that the velocity field plays an important and completely independent role in the spatial description. Indeed, in contrast to the material description, which is based on two position vectors (the reference one and the current one), the spatial description is based on using the velocity vector along with the current position vector. Therefore, in the spatial description, it is of interest to determine the strain measures by means of the equations relating them to the velocity gradient, but not to the displacement gradient. These equations are well known, see, e.g., [28,29,37]. They have exactly the same structure in both the descriptions. The only difference is that we employ the total time derivative in the material description and the material time derivative in the spatial description, see [38,39].

We emphasize that it is not advisable to use the equations directly relating the strain measures to the velocity gradient in the material description. However, these equations turn out to be very useful in the spatial description. First of all, they allow us to close the system of differential equations without using the displacement vector, see [29]. In addition, they allow us to look at the strain measures as parameters of state in the broadest sense, and not as the purely geometrical characteristics. The latter may open a way to modify the strain measure definition. This, in turn, may open up new prospects for describing the processes connected with the substance supply.

The main objective of our study is to analyze the differential equation relating the strain measure to the velocity gradient and to reduce this equation to the integral form, or rather to the form of the balance equation. The novelty consists in the modification of the obtained balance equation by adding a source term into it. We note that equations for strain measures having the form of the balance equation can be found in [24,37,40], but the corresponding equation with the source term is suggested for the first time. We believe that this equation may be useful for describing various structural transformations and phase transitions in solids, as well as chemical reactions in multi-component media. This source term can also be used to simulate the processes associated with the substance supply not through the surface, but directly into the volume, e.g., by means of a syringe. It is obvious that the process of the substance supply depends on the direction of the syringe needle. It is also obvious that this process cannot be modeled with the sufficient accuracy if only the source term in the mass balance equation is used, because the scalar source term does not allow one to take into account the syringe needle direction. We note that we can consider the substance supply directly into the volume regardless of whether this substance is a fluid or a solid. Certainly, it is difficult to imagine the supply of solids with a syringe. But we can consider the supply of a fluid that instantly turns into a solid under the certain thermal or chemical conditions. Simulating this process, we can assume that we supply the solid with a syringe. Below we discuss two examples of solid deformation caused by the source term in the equation for the strain measure.

The partial differential equations obtained via the spatial description are usually discretized by using the Finite Volume Method (FVM), see [14,41–44]. Certainly, the numerical methods based on the spatial description, including the FVM, have their advantages and disadvantages. In particular, it is problematic to formulate the Dirichlet–Neumann boundary conditions in the case of the moving boundary of matter using these methods. That is why the hybrid approaches are often used. They possess the advantages of the both material and spatial descriptions and reduce the inconveniences of each one. Some cutting edge numerical techniques based on such approaches has been firstly developed in fluid dynamics and later on adapted to solid mechanics. One of these methods we employ in this paper. This method consists in the following. We use the spatial description to formulate all the differential equations in the whole computational domain. An important and innovative aspect of our approach is to use the components of the inverse deformation gradient as the main variables. To be precise, we eliminate the components of the displacement vector and obtain the differential equations that directly relate the components of the velocity vector and the components of the inverse deformation gradient. On the one hand, these differential equations play the role of the kinematics relations, because they do not contain any material constants. On the other hand, these differential equations can be interpreted as generalizations of the mass balance equation, since the latter can be rewritten in terms of the determinant of the inverse deformation gradient. Thus, we obtain the system of differential equations describing the behavior of solids that has the same structure as the system of differential equations in the gas and fluid dynamics. The only difference is that, in the case of gas and fluid, the system of equations includes the mass balance equation, whereas we use equations relating the velocities and strains. Along with the spatial description, we also apply the material description, but only to track the interface of the material. Using this hybrid description allows one to formulate various conditions at the cells where the interface of the material is located at the given moments of time. For example, one can apply the Dirichlet–Neumann conditions to the moving boundary of the material. We employ the front tracking technique to locate the interface of the material, see [45]. In accordance to this technique, we interpolate the velocity field at points located in close proximity to the interface of the material and in this manner we calculate the velocities of the interface points. After that we use these velocities for determining the position of the interface of the material at the next moment of time. We discretize the system of the differential equations using the Finite Volume Method and explicit time integration scheme, as it is usually done in the fluid and gas dynamics. We note that our program allows us to use a highly irregular mesh for space discretization. We also can solve problems for solids of any shape, because the program performs a set of boolean operations to construct the initial map of the density. But the main advantage of our approach is that it makes it possible to simulate the non-isotropic supply of matter by means of source terms in the differential equations for the strains.

2 The solid mechanics problems in the spatial description

Below we consider the solid mechanics problems and apply the spatial (Eulerian) description. Let vector $\mathbf{r}$ identify the position of the center of a control volume. Then, all variables characterizing the stress–strain state of the matter are the functions of position vector $\mathbf{r}$ and time t. We use the following notations: $\mathbf{v} = \mathbf{v}(\mathbf{r}, t)$ is the velocity vector field; $\rho = \rho(\mathbf{r}, t)$ is the density field; $\boldsymbol{\sigma} = \boldsymbol{\sigma}(\mathbf{r}, t)$ is the Cauchy stress tensor; $\mathbf{g} = \mathbf{g}(\mathbf{r}, t)$ is the inverse deformation gradient; and $U = U(\mathbf{r}, t)$ is the internal energy per unit mass.

2.1 The total time derivative and the material time derivative

Now we consider a moving control volume (or, what is the same thing, a moving observation point). A position of the observation point in a reference frame is determined by position vector $\mathbf{r}(x, y, z, t)$, where x, y, z are the reference coordinates. Velocity of the observation point $\mathbf{v}_O$ is calculated as $\mathbf{v}_O = \dfrac{d\mathbf{r}}{dt}$ or as $\mathbf{v}_O = \dfrac{\partial \mathbf{r}}{\partial t}$, what is the same thing since coordinates x, y, z do not depend on time. We suppose that a matter flows through the control volume. At time t, some part of the matter occupies the control volume. This part of the matter possesses velocity $\mathbf{v}$. We emphasize that $\mathbf{v} \neq \mathbf{v}_O$. At time $t + \Delta t$, the position of the observation point is identified by position vector $\mathbf{r} + \mathbf{v}_O \Delta t$ and the considered part of the matter occupies a new control volume, the position of which is identified by position vector $\mathbf{r} + \mathbf{v} \Delta t$.

Next, we consider scalar function $f = f(\mathbf{r}, t)$ characterizing a property of the matter or a process in the matter.

The total time derivative determines the rate of change of function f in the given control volume at the given time. It is defined as

$$\frac{\mathrm{d}f}{\mathrm{d}t} = \lim_{\Delta t \to 0} \frac{f(\mathbf{r} + \mathbf{v}_O \Delta t, t + \Delta t) - f(\mathbf{r}, t)}{\Delta t}. \tag{1}$$

It is obvious that different parts of the matter occupy the given control volume at different time. That is why, the total time derivative characterizes the process at the given point of space rather than at the given part of the matter.

The material time derivative determines the rate of change of characteristic f associated with that part of the matter which turns out in the given point of space at the given moment of time. It is defined by the following formula [28,38]:

$$\frac{\delta f}{\delta t} = \lim_{\Delta t \to 0} \frac{f(\mathbf{r} + \mathbf{v} \Delta t, t + \Delta t) - f(\mathbf{r}, t)}{\Delta t}. \tag{2}$$

The expression on the right-hand side of Eq. (2) can be divided into two parts as

$$\frac{\delta f}{\delta t} = \lim_{\Delta t \to 0} \frac{f(\mathbf{r} + \mathbf{v}_O \Delta t, t + \Delta t) - f(\mathbf{r}, t)}{\Delta t} + \\ + \lim_{\Delta t \to 0} \frac{f(\mathbf{r} + \mathbf{v} \Delta t, t + \Delta t) - f(\mathbf{r} + \mathbf{v}_O \Delta t, t + \Delta t)}{\Delta t} \tag{3}$$

The first term on the right-hand side of Eq. (3) is the total time derivative, see Eq. (1). The second term on the right-hand side of Eq. (3) is the convective derivative. It is related to the rate of change of characteristic f due to the fact that the given part of the matter moves with velocity $\mathbf{v} - \mathbf{v}_O$ relative to the control volume and occupies different control volumes at the subsequent moments of time. Thus, the material time derivative is defined as

$$\frac{\delta f}{\delta t} = \frac{\mathrm{d}f}{\mathrm{d}t} + (\mathbf{v} - \mathbf{v}_O) \cdot \nabla f, \qquad \nabla = \frac{\partial}{\partial \mathbf{r}}. \tag{4}$$

We note that in the case of the material description the observation point moves with the material volume. This means that

$$\mathbf{v}_O = \mathbf{v} \quad \Rightarrow \quad \frac{\delta f}{\delta t} = \frac{\mathrm{d}f}{\mathrm{d}t}. \tag{5}$$

In hydrodynamics, the fixed observation point is usually used. In this case

$$\mathbf{v}_O = 0 \quad \Rightarrow \quad \frac{\delta f}{\delta t} = \frac{\mathrm{d}f}{\mathrm{d}t} + \mathbf{v} \cdot \nabla f. \tag{6}$$

In this section, we have considered the moving observation point in order to clarify the difference between the total time derivative and the material time derivative. We emphasize that below we use the spatial description, and hence, we use the material derivatives. Below, for simplicity sake, we consider the fixed observation point.

2.2 The mass balance equation

Let us consider an open control volume V fixed in the reference frame and bounded by surface S. In general case, the mass change inside the control volume can be caused by two different processes: the mass flow through the surface and the supply of mass to the volume. The integral form of the mass balance equation is well known:

$$\frac{\mathrm{d}}{\mathrm{d}t} \int_V \rho \mathrm{d}V = - \int_S (\mathbf{n} \cdot \mathbf{v}) \rho \, \mathrm{d}S + \int_V \chi_\rho \mathrm{d}V, \tag{7}$$

where $\mathbf{n}$ denotes the outward-pointing unit normal vector to surface S, and χ_ρ is the mass supply per unit volume per unit time. We can consider Eq. (7) as the mass balance equation for one of the mixture components. In this case, the source term χ_ρ characterizes the mass exchange between the components of the mixture due to chemical reactions or some mechanical processes such as adhesion of particles of one component to particles of another component. We can also use the source term χ_ρ to simulate various mechanical processes, e.g., the Hele–Shaw flows, where the mass is supplied with a syringe in the direction perpendicular to the flow plane, or even biological processes like the volume growth of tumors due to the anomalous cell division [46], as well as many other processes.

It is well known that from Eq. (7) it follows the local form of the mass balance equation

$$\frac{\delta \rho}{\delta t} + \rho \nabla \cdot \mathbf{v} = \chi_\rho, \tag{8}$$

where the material derivative is defined by Eq. (6). We note that if $\chi_\rho = 0$ the whole system is a closed system, certainly under the appropriate boundary conditions, whereas the infinitesimal control volume is an opened system in any case.

2.3 The linear momentum balance equation

The integral form of the linear momentum balance equation is

$$\frac{\mathrm{d}}{\mathrm{d}t} \int_V \rho \mathbf{v} \mathrm{d}V = - \int_S (\mathbf{n} \cdot \mathbf{v}) \rho \mathbf{v} \mathrm{d}S + \int_S \mathbf{n} \cdot \boldsymbol{\sigma} \, \mathrm{d}S + \int_V \rho \mathbf{f} \mathrm{d}V + \int_V \chi_\rho \mathbf{v}_* \mathrm{d}V. \tag{9}$$

Here $\mathbf{f}$ is the body force, $\mathbf{v}_*$ is the velocity of particles of the supplied matter. Velocity $\mathbf{v}_*$ can be equal to zero, e.g., if we model the adhesion of particles of a stationary medium to particles of a moving medium. Velocity $\mathbf{v}_*$ can be equal to velocity $\mathbf{v}$, e.g., if we model chemical reactions in a mixture, all components of which move at the same velocity. In view of Eqs. (6), (8), from Eq. (9) one can obtain the local form of the linear momentum balance equation

$$\rho \frac{\delta \mathbf{v}}{\delta t} = \nabla \cdot \boldsymbol{\sigma} + \rho \mathbf{f} + \chi_\rho (\mathbf{v}_* - \mathbf{v}). \tag{10}$$

We note that source term $\chi_\rho (\mathbf{v}_* - \mathbf{v})$ in Eq. (10) can be treated as an internal body force, see [18]. We believe that this is a question of terminology, and nothing more.

When using the spatial description, the boundary conditions are formulated only at the boundary of the computational domain. Let us assume that the computational domain is not completely filled with a material. In this case, there are boundaries between the material under consideration and empty space (or some other material) within the computational domain. Let us assume that some external forces are distributed over the surface of these internal boundaries of the material. Within the framework of the spatial description, we cannot formulate the boundary conditions at these internal boundaries. Hence, we should replace these surface forces with the corresponding body forces in the momentum balance equation. Thus, it is convenient to represent the body force $\mathbf{f}$ in Eq. (10) as the sum of two terms, namely

$$\mathbf{f} = \mathbf{f}_b + \mathbf{f}_c, \tag{11}$$

where $\mathbf{f}_b$ is the true body force, e.g., gravity force, and $\mathbf{f}_c$ is the body force modeling some surface forces, e.g., the Neumann boundary conditions, see [24,47]. Substituting Eq. (11) into Eq. (10) yields

$$\rho \frac{\delta \mathbf{v}}{\delta t} = \nabla \cdot \boldsymbol{\sigma} + \rho \mathbf{f}_b + \rho \mathbf{f}_c + \chi_\rho (\mathbf{v}_* - \mathbf{v}). \tag{12}$$

Later on, we discuss in more detail how to change the surface force by the equivalent body force $\rho \mathbf{f}_c$.

2.4 The angular momentum balance equation

We assume that the rotational degree of freedom and the moment interactions are absent. Then, the integral form of the angular momentum balance equation is

$$
\frac{\mathrm{d}}{\mathrm{d}t} \int_V \mathbf{r} \times (\rho \mathbf{v}) \mathrm{d}V = - \int_S (\mathbf{n} \cdot \mathbf{v}) \, \mathbf{r} \times (\rho \mathbf{v}) \mathrm{d}S + \int_S \mathbf{r} \times (\mathbf{n} \cdot \boldsymbol{\sigma}) \mathrm{d}S +
$$
$$
+ \int_V \mathbf{r} \times \rho \mathbf{f} \mathrm{d}V + \int_V \mathbf{r} \times \chi_\rho \mathbf{v}_* \mathrm{d}V
\tag{13}
$$

Transformation of Eq. (13) in view of Eqs. (4), (8), (10) yields $\boldsymbol{\sigma} = \boldsymbol{\sigma}^{\mathrm{T}}$. Thus, we see that the stress tensor must be symmetric even if the mass supply is taken into account.

2.5 Differential and integral equations for the strain measure

It is well known that, in the material description, the inverse deformation gradient $\mathbf{g}$ is defined as

$$
\mathbf{g} = \mathbf{E} - \nabla \mathbf{u},
\tag{14}
$$

where $\mathbf{E}$ is the second-rank identity tensor, ∇ is the gradient operator at the current configuration, $\mathbf{u}$ is the displacement vector. Exactly the same strain measure can be introduced in the spatial description, see, e.g., [25,28,29].

Below we use only the spatial description. As shown in [29], in the spatial description, the displacement vector does not have a clear geometrical meaning. In fact, we can consider the relation between the displacement vector and the velocity vector

$$
\frac{\delta \mathbf{u}}{\delta t} = \mathbf{v}
\tag{15}
$$

as the definition of the displacement vector. Such definition can be found in [29]. Certainly, this is not the only possible definition of the displacement vector in a spatial description. We can consider Eq. (14) as an alternative definition of the displacement vector if we define tensor $\mathbf{g}$ by means of an equation that directly relates it to the velocity gradient. In Sect. 2.8, we discuss two definitions of the displacement vector in more detail.

It is evident that one can exclude vector $\mathbf{u}$ from the system of Eqs. (14), (15) and obtain a differential equation that directly relates the strain measure to the velocity gradient. First of all, we refer to [25,28,29], where this equation is given in the form

$$
\frac{\delta \mathbf{g}}{\delta t} = -(\nabla \mathbf{v}) \cdot \mathbf{g}.
\tag{16}
$$

In addition, we note that it is not difficult to show that Eq. (16) can be rewritten as

$$
\frac{\delta \mathbf{g}^{-1}}{\delta t} = \mathbf{g}^{-1} \cdot (\nabla \mathbf{v}).
\tag{17}
$$

Next, we consider another form of the differential equation relating the strain measure to the velocity gradient. In view of Eq. (4), we rewrite Eq. (15) as

$$
\frac{\mathrm{d}\mathbf{u}}{\mathrm{d}t} = \mathbf{v} \cdot (\mathbf{E} - \nabla \mathbf{u}),
\tag{18}
$$

Taking the gradient of both sides of Eq. (18) and changing the order of the gradient operator and the total time derivative, we obtain

$$
\frac{\mathrm{d}(\nabla \mathbf{u})}{\mathrm{d}t} = \nabla \big(\mathbf{v} \cdot [\mathbf{E} - \nabla \mathbf{u}] \big).
\tag{19}
$$

Taking into account the definition of the strain measure (14), we can rewrite Eq. (19) as

$$
\frac{\mathrm{d}\mathbf{g}}{\mathrm{d}t} = -\nabla (\mathbf{v} \cdot \mathbf{g}).
\tag{20}
$$

Equation (20) is less known than Eqs. (16), (17), but it also can be found in literature, see, e.g., [37,40]. Certainly, Eqs. (16), (17), (20) are equivalent to each other.

Generally speaking, we can consider any of Eqs. (16), (17), (20) as the definition of strain measure $\mathbf{g}$. To be exact, we can replace the definition of the strain measure (18) with any of the listed equations. In this manner we can obtain a closed system of the differential equations describing dynamical processes in solids, in which tensor $\mathbf{g}$ will play the role of one of the main variables and vector $\mathbf{u}$ will be absent. Thus, if we do not need the displacement vector, we can ignore both Eqs. (14), (15). If we still need vector $\mathbf{u}$, it can be calculated by using any of Eqs. (14), (15) when tensor $\mathbf{g}$ and vector $\mathbf{v}$ are already known. The possibility of using Eq. (15) does not need proof. The possibility of using Eq. (14) is less obvious. Let us prove this. First of all, we note that from Eq. (20) it follows that $\dfrac{d}{dt}(\nabla \times \mathbf{g}) = 0$. Hence, if $(\nabla \times \mathbf{g})|_{t=0} = 0$, then $\nabla \times \mathbf{g} = 0$. Hence, $\nabla \times (\mathbf{E} - \mathbf{g}) = 0$. This means that tensor $\mathbf{E} - \mathbf{g}$ can be represented as $\nabla \mathbf{u}$. Thus, Eq. (14) has a solution for any tensor $\mathbf{g}$ satisfying Eq. (20).

We note that Eq. (20) essentially differs from Eqs. (16), (17), because it can be rewritten in the integral form. Indeed, integrating Eq. (20) over the volume and applying the divergence theorem, we have

$$\frac{\mathrm{d}}{\mathrm{d}t} \int_V \mathbf{g}\mathrm{d}V = - \int_S \mathbf{n}(\mathbf{v} \cdot \mathbf{g})\mathrm{d}S. \tag{21}$$

Now we introduce a third-rank tensor

$$\mathbf{J}_g = \mathbf{E}\,\mathbf{v} \cdot \mathbf{g}. \tag{22}$$

In view of Eq. (22), we can rewrite Eq. (21) as

$$\frac{\mathrm{d}}{\mathrm{d}t} \int_V \mathbf{g}\mathrm{d}V = - \int_S \mathbf{n} \cdot \mathbf{J}_g \mathrm{d}S. \tag{23}$$

It is evident that Eq. (23) has the structure of the integral balance equation and tensor $\mathbf{J}_g$ can be treated as the strain flow tensor. We believe that Eq. (23) is of interest. On the one hand, it is convenient to use this equation when solving problems numerically via finite volume method. Such an approach was developed in [24,37]. On the other hand, Eq. (23) suggests that it is possible to modify the definition of the strain measure. This can be useful for modeling processes where the mass supply from the external source is taken into account.

2.6 The mass density and the determinant of the strain measure

It is well known that, in gas and fluid dynamics, the mass density is one of the main variables and the mass balance equation is one of the basic equations. If the source term is absent, this equation takes the form

$$\frac{\delta \rho}{\delta t} + \rho \, \nabla \cdot \mathbf{v} = 0. \tag{24}$$

In solid mechanics, Eq. (24) is not included into the system of the basic equations, if the material description is used. In this case the current value of the mass density is calculated by the algebraic formula relating it to its reference value and the volumetric strain. Exactly the same algebraic relation holds in the spatial description, if the source term in the mass balance equation is absent. This relation has the form

$$\rho = \rho_0 \, I_3(\mathbf{g}), \qquad I_3(\mathbf{g}) \equiv \mathrm{Det}\,\mathbf{g}, \tag{25}$$

where I_3 determines the volume strain of the matter, ρ_0 is the value of ρ corresponding to the unstrained state of the matter, i.e., the state when $\mathbf{g} = \mathbf{E}$, and hence, $I_3 = 1$. A substantiation of Eq. (25) is as follows. As shown, e.g., in [28], from Eq. (16) it follows that

$$\frac{\delta I_3}{\delta t} + I_3 \, \nabla \cdot \mathbf{v} = 0, \tag{26}$$

and from Eqs. (24), (26) it follows that

$$\frac{1}{\rho} \frac{\delta \rho}{\delta t} = \frac{1}{I_3} \frac{\delta I_3}{\delta t} \qquad \Rightarrow \qquad \frac{\delta}{\delta t}\left(\frac{\rho}{I_3}\right) = 0. \tag{27}$$

It is evident that Eq. (25) is a solution of Eq. (27). Although, as shown in [28], Eq. (27) has other solutions. But we will not discuss them here.

Now we consider the dynamical processes when it is necessary to take into account the source term in the mass balance equation. In other words, we return to Eq. (8). There are two possibilities.

1. We can keep the generally accepted definition of the strain measure or, that is the same thing, the definition of the strain measure in the form of Eq. (20). Then, Eq. (26) remains unchanged. In this case, we reject Eq. (25) relating the density of matter to its volume strain.
2. We can keep Eq. (25). In this case we are forced to add the corresponding source term into Eq. (26). This means that we need to modify the definition of the strain measure by adding a source term to it.

In our study, we choose the second way, i.e., we add the source term into the equation for strains. Then, the equation for I_3 takes the form

$$\frac{\delta I_3}{\delta t} + I_3 \nabla \cdot \mathbf{v} = \chi_3. \tag{28}$$

In order to keep Eq. (25) unchanged, source terms χ_ρ and χ_3 must be related as

$$\chi_\rho = \chi_3 \frac{\rho}{I_3}. \tag{29}$$

2.7 The strain balance equation with the source term

It is obvious that we cannot replace Eq. (26) with Eq. (28), keeping the equation for tensor $\mathbf{g}$ unchanged. As mentioned above, the differential equation for tensor $\mathbf{g}$ can be written in different forms, e.g., Eqs. (16), (17), (20). Looking at the problem from a purely mathematical point of view, we conclude that one can add source terms to all of the listed equations. It is obvious that the source terms will be related to each other. But it is not obvious whether the source terms will have a clear physical meaning. The situation becomes quite different when we consider the integral form of the equation for tensor $\mathbf{g}$, namely Eq. (23). Since it has the form of the balance equation, adding the source term to this equation, we take into account the supply of strains to the control volume.

Thus, adding of source term $\boldsymbol{\chi}_g$ to Eq. (23) yields

$$\frac{\mathrm{d}}{\mathrm{d}t} \int\limits_V \mathbf{g}\, \mathrm{d}V = -\int\limits_S \mathbf{n} \cdot \mathbf{J}_g\, \mathrm{d}S + \int\limits_V \boldsymbol{\chi}_g\, \mathrm{d}V. \tag{30}$$

From Eqs. (22), (30) it follows the local form of the strain balance equation

$$\frac{\mathrm{d}\mathbf{g}}{\mathrm{d}t} = -\nabla(\mathbf{v} \cdot \mathbf{g}) + \boldsymbol{\chi}_g. \tag{31}$$

2.8 Two definitions of the displacement vector

Now we turn to the definition of the displacement vector. As shown above, Eq. (20) follows from Eqs. (14), (15). It is evident that, if we change Eq. (20) by adding source term $\boldsymbol{\chi}_g$, i.e, we replace Eq. (20) with Eq. (31), then both equations (14), (15) cannot hold true simultaneously. We can reject one of Eqs. (14), (15) and use the other one as the definition of the displacement vector. We consider two approaches.

Approach 1. We reject Eq. (14) and define the displacement vector by means of Eq. (15). In this case, source term $\boldsymbol{\chi}_g$ can be chosen arbitrary. From Eq. (31) it follows

$$\frac{\delta \mathbf{g}}{\delta t} = -(\nabla \mathbf{v}) \cdot \mathbf{g} + \mathbf{v} \cdot \nabla \mathbf{g} - (\nabla \mathbf{g}^{\mathrm{T}}) \cdot \mathbf{v} + \boldsymbol{\chi}_g. \tag{32}$$

We emphasize that if we reject Eq. (14) we cannot prove that terms $\mathbf{v} \cdot \nabla \mathbf{g}$ and $(\nabla \mathbf{g}^{\mathrm{T}}) \cdot \mathbf{v}$ are equal to each other. That is why, Eq. (32) differs from Eq. (16) not only by term $\boldsymbol{\chi}_g$, but also by two additional terms. From Eq. (32) we obtain

$$\frac{\delta I_3}{\delta t} + I_3 \left(\nabla \cdot \mathbf{v} + \mathbf{g}^{-1} \cdot \cdot (\nabla \mathbf{g}^{\mathrm{T}}) \cdot \mathbf{v} - \mathbf{v} \cdot (\nabla \mathbf{g}) \cdot \cdot \mathbf{g}^{-1} \right) = \chi_3, \tag{33}$$

where

$$\chi_3 = I_3 \mathbf{g}^{-1} \cdot \cdot \boldsymbol{\chi}_g. \tag{34}$$

It is easy to see that Eq. (33) differs from Eq. (28). This means that we cannot keep Eq. (25) unchanged even if source terms χ_ρ and χ_3 are related by Eq. (29).

Approach 2. We reject Eq. (15) and use Eq. (14) to define the displacement vector. In this case, we have the following restriction:

$$\nabla \times \mathbf{g} = 0. \tag{35}$$

It is not difficult to show that from Eqs. (31), (35) it follows that

$$\nabla \times \boldsymbol{\chi}_g = 0. \tag{36}$$

In view of Eq. (14), from Eq. (31) we obtain

$$\frac{\delta \mathbf{g}}{\delta t} = -(\nabla \mathbf{v}) \cdot \mathbf{g} + \boldsymbol{\chi}_g. \tag{37}$$

It is evident that Eq. (37) differs from Eq. (16) only by the additional term $\boldsymbol{\chi}_g$. From Eq. (37) it follows Eq. (28), where source term χ_3 is given by Eq. (34). Hence, Eq. (25) is hold true and source term χ_ρ can be expressed through source term χ_3 by Eq. (29). From Eqs. (29), (34) it follows that χ_ρ can be calculated as

$$\chi_\rho = \rho \, \mathbf{g}^{-1} \cdot \cdot \boldsymbol{\chi}_g. \tag{38}$$

In addition, we note that, in the considered case, we can replace Eq. (15) by the equation

$$\frac{\delta \mathbf{u}}{\delta t} = \mathbf{v} + \boldsymbol{\chi}_u, \tag{39}$$

where $\boldsymbol{\chi}_u$ is a source term. We can prove this by the following line of reasoning. In view of Eq. (14), we rewrite Eq. (39) as

$$\frac{d \mathbf{u}}{d t} = \mathbf{v} \cdot (\mathbf{E} - \nabla \mathbf{u}) + \boldsymbol{\chi}_u. \tag{40}$$

Next, taking the gradient operator of the both sides of Eq. (40) and taking into account Eq. (14), we obtain

$$\frac{d \mathbf{g}}{d t} = -\nabla (\mathbf{v} \cdot \mathbf{g}) - \nabla \boldsymbol{\chi}_u. \tag{41}$$

Comparing Eq. (41) with Eq. (31) we conclude that

$$\boldsymbol{\chi}_g = -\nabla \boldsymbol{\chi}_u. \tag{42}$$

It is easy to see that source term $\boldsymbol{\chi}_g$ defined by Eq. (42) identically satisfies the restriction given by Eq. (36). Thus, we have proved that if we introduce the source term in the strain balance equation and define the displacement vector by Eq. (14), we can replace Eq. (15) by Eq. (39).

Now we cannot say that one of two considered approaches is preferable to the other. Perhaps the choice of approach depends on the problem being solved.

2.9 The strain balance equation and the mass balance equation

We note that adding the source term to the equation for the strain measure we change the definition of the strain measure and endow the strain measure with new physical meaning. In fact, we can consider Eq. (31) as a new definition of the strain measure. If we look at the strain measure from the point of view of its new definition, we can return to the question of whether the mass density and the determinant of the strain must be related. There are two possibilities.

1. We can use Eq. (38) for calculating the source term in the mass balance equation. In this case ρ will be related to the determinant of $\mathbf{g}$ by Eq. (25).
2. We can reject Eqs. (38). In this case we can consider $\mathbf{g}$ and ρ as the independent variables.

In this study, we choose the first approach. However, we believe that the second approach can be useful when modeling phase transitions and structural transformations that result in changes of some mechanical characteristics of solids, but do not result in change of the mass density. For modeling such processes, we can use the strain balance equation with the source term and the mass balance equation without the source term.

2.10 The energy balance equation in the simplest case

Now we consider the purely mechanical processes. Thus, we assume that the supply of thermal, electrical, chemical and other non-mechanical energy is absent. However, we take into account the mass supply. Certainly, the supplied substance can possess both the kinetic energy and the internal energy. In view of the aforesaid, the energy balance equation is written as

$$\frac{\mathrm{d}}{\mathrm{d}t} \int_V \rho \left(\frac{1}{2}\mathbf{v} \cdot \mathbf{v} + U\right) \mathrm{d}V = \int_S (\mathbf{n} \cdot \boldsymbol{\sigma}) \cdot \mathbf{v}\mathrm{d}S + \int_V \rho\mathbf{f} \cdot \mathbf{v}\mathrm{d}V -$$
$$- \int_S (\mathbf{n} \cdot \mathbf{v})\rho \left(\frac{1}{2}\mathbf{v} \cdot \mathbf{v} + U\right) \mathrm{d}S + \int_V \left(\frac{1}{2}\chi_\rho\mathbf{v}_* \cdot \mathbf{v}_* + \chi_e\right) \mathrm{d}V, \tag{43}$$

where χ_e is the internal energy of the supplied substance per unit volume per unit time. Applying the divergence theorem and taking into account Eqs. (4), (8), (10), after some transformations we obtain

$$\rho\frac{\delta U}{\delta t} = \boldsymbol{\sigma}^{\mathrm{T}} \cdot \cdot (\nabla\mathbf{v}) + \frac{1}{2}\chi_\rho(\mathbf{v}_* - \mathbf{v})^2 + \chi_e - \chi_\rho U. \tag{44}$$

Now we should eliminate $\nabla\mathbf{v}$ from Eq. (44) in view of Eq. (32) or Eq. (37). Let us use, e.g., Eq. (37). Then we reduce Eq. (44) to the form

$$\rho\frac{\delta U}{\delta t} = -\boldsymbol{\sigma}^{\mathrm{T}} \cdot \cdot \left(\frac{\delta\mathbf{g}}{\delta t} \cdot \mathbf{g}^{-1}\right) + \left[\frac{1}{2}\chi_\rho(\mathbf{v}_* - \mathbf{v})^2 + \chi_e - \chi_\rho U + \boldsymbol{\sigma} \cdot \cdot \left(\boldsymbol{\chi}_g \cdot \mathbf{g}^{-1}\right)\right]. \tag{45}$$

For simplicity sake, we assume that

$$\chi_e = \chi_\rho U - \frac{1}{2}\chi_\rho(\mathbf{v}_* - \mathbf{v})^2 - \boldsymbol{\sigma} \cdot \cdot (\boldsymbol{\chi}_g \cdot \mathbf{g}^{-1}). \tag{46}$$

In view of Eq. (46), the energy balance equation (45) takes the form

$$\rho\frac{\delta U}{\delta t} = -\boldsymbol{\sigma}^{\mathrm{T}} \cdot \cdot \left(\frac{\delta\mathbf{g}}{\delta t} \cdot \mathbf{g}^{-1}\right). \tag{47}$$

2.11 The constitutive equation for the stress tensor

In order to derive the constitutive equation, we perform the standard transformations of Eq. (47) taking into account the fact that tensor $\boldsymbol{\sigma}$ is the symmetric one. As a result, we obtain

$$\rho\frac{\delta U}{\delta t} = \left(\mathbf{g} \cdot \boldsymbol{\sigma} \cdot \mathbf{g}^{\mathrm{T}}\right) \cdot \cdot \frac{\delta\mathbf{e}}{\delta t}, \tag{48}$$

where $\mathbf{e}$ is the Green strain tensor, which has the form

$$\mathbf{e} = \frac{1}{2}(\mathbf{g}^{-T} \cdot \mathbf{g}^{-1} - \mathbf{E}). \tag{49}$$

We assume the material to be elastic. Then, in accordance with Eq. (48), the internal energy U is a function of tensor $\mathbf{e}$. Substituting $U = U(\mathbf{e})$ into Eq. (48) and taking into account Eq. (25) yields

$$\boldsymbol{\sigma} = \det(\mathbf{g})\,\mathbf{g}^{-1} \cdot \frac{\partial(\rho_0 U)}{\partial\mathbf{e}} \cdot \mathbf{g}^{-T}. \tag{50}$$

Thus, Eq. (50) allows us to represent the stress tensor in terms of strain measure $\mathbf{g}$ if the internal energy is specified as the function of tensor $\mathbf{e}$.

For simplicity sake, we consider the physically linear isotropic elastic material. We use the St.Venant–Kirchhoff model:

$$\rho_0 U = \frac{\lambda}{2}\,\mathrm{tr}^2(\mathbf{e}) + \mu\mathbf{e} \cdot \cdot \mathbf{e}, \tag{51}$$

where λ and μ are the Lame parameters. Substituting Eq.(52) into Eq.(50), we obtain the constitutive equation

$$\boldsymbol{\sigma} = \det(\mathbf{g})\,\mathbf{g}^{-1} \cdot (\lambda\,\mathrm{tr}(\mathbf{e})\mathbf{E} + 2\mu\mathbf{e}) \cdot \mathbf{g}^{-T}. \tag{52}$$

2.12 Description of thermal processes in view of the new concept of strains

Now we rewrite the energy balance equation (43) taking into account thermal processes. We have

$$
\begin{aligned}
\frac{\mathrm{d}}{\mathrm{d}t} \int_V \rho \left(\frac{1}{2} \mathbf{v} \cdot \mathbf{v} + U \right) \mathrm{d}V &= \int_S (\mathbf{n} \cdot \boldsymbol{\sigma}) \cdot \mathbf{v} \mathrm{d}S + \int_V \rho \mathbf{f} \cdot \mathbf{v} \mathrm{d}V - \int_S \mathbf{n} \cdot \mathbf{h} \, \mathrm{d}S \\
&+ \int_V \rho q \, \mathrm{d}V - \int_S (\mathbf{n} \cdot \mathbf{v}) \rho \left(\frac{1}{2} \mathbf{v} \cdot \mathbf{v} + U \right) \mathrm{d}S + \int_V \left(\frac{1}{2} \chi_\rho \mathbf{v}_* \cdot \mathbf{v}_* + \chi_e \right) \mathrm{d}V.
\end{aligned}
\tag{53}
$$

Here $\mathbf{h}$ is the heat flux vector, q is the heat supply from the external source per unit mass per unit time. In view of Eqs. (4), (8), (10), (37), from Eq. (53) it follows

$$
\begin{aligned}
\rho \frac{\delta U}{\delta t} &= -\boldsymbol{\sigma}^T \cdot \cdot \left(\frac{\delta \mathbf{g}}{\delta t} \cdot \mathbf{g}^{-1} \right) - \nabla \cdot \mathbf{h} + \rho q \\
&+ \left[\frac{1}{2} \chi_\rho (\mathbf{v}_* - \mathbf{v})^2 + \chi_e - \chi_\rho U + \boldsymbol{\sigma} \cdot \cdot \left(\boldsymbol{\chi}_g \cdot \mathbf{g}^{-1} \right) \right].
\end{aligned}
\tag{54}
$$

For simplicity sake, we assume the material to be elastic. Next, we introduce the absolute temperature T and the entropy per unit mass $\mathcal{H}$ in the same way as it is done in [25–28]:

$$
\rho T \frac{\delta \mathcal{H}}{\delta t} = -\nabla \cdot \mathbf{h} + \rho q + \left[\frac{1}{2} \chi_\rho (\mathbf{v}_* - \mathbf{v})^2 + \chi_e - \chi_\rho U + \boldsymbol{\sigma} \cdot \cdot \left(\boldsymbol{\chi}_g \cdot \mathbf{g}^{-1} \right) \right].
\tag{55}
$$

In view of Eq. (55) the energy balance equation takes the form

$$
\rho \frac{\delta U}{\delta t} = -\boldsymbol{\sigma}^{\mathrm{T}} \cdot \cdot \left(\frac{\delta \mathbf{g}}{\delta t} \cdot \mathbf{g}^{-1} \right) + \rho T \frac{\delta \mathcal{H}}{\delta t}.
\tag{56}
$$

Equation (56) is called the reduced energy balance equation. It allows to obtain the constitutive equations for stress tensor $\boldsymbol{\sigma}$ and temperature T. Equation (55) is the heat conduction equation. We pay attention to two important facts. Firstly, source term $\boldsymbol{\chi}_g$ effects thermal processes. Secondly, if source term $\boldsymbol{\chi}_g$ is not equal to zero, then an additional effect of elastic stresses on thermal processes appears. This additional effect is not directly related to the thermal expansion.

Here we briefly outline a way that allows us to describe the mutual influence of thermal and mechanical processes in view of our concept of strains. A more detailed discussion of this subject is beyond the scope of this study. But we note that our approach can be useful, e.g., in describing structural transformations in metals that occur as a result of mechanical and thermal effects. It also can be useful in describing the processes of crushing rocks.

3 Computational aspects

To solve the problems numerically, we use the finite volume method. Therefore, we formulate the basic equations in the integral form, namely

$$
\begin{aligned}
\frac{\mathrm{d}}{\mathrm{d}t} \int_V \rho \mathbf{v} \mathrm{d}V &= -\int_S (\mathbf{n} \cdot \mathbf{v}) \rho \mathbf{v} \mathrm{d}S + \int_S \mathbf{n} \cdot \boldsymbol{\sigma} \mathrm{d}S + \int_V \rho \mathbf{f} \mathrm{d}V + \int_V \chi_\rho \mathbf{v}_* \mathrm{d}V, \\
\frac{\mathrm{d}}{\mathrm{d}t} \int_V \rho \mathrm{d}V &= -\int_S \mathbf{n} \cdot (\rho \mathbf{v}) \mathrm{d}S + \int_V \chi_\rho \mathrm{d}V, \\
\frac{\mathrm{d}}{\mathrm{d}t} \int_V \mathbf{g} \mathrm{d}V &= -\int_S \mathbf{n} \cdot \mathbf{J}_g \, \mathrm{d}S + \int_V \boldsymbol{\chi}_g \, \mathrm{d}V.
\end{aligned}
\tag{57}
$$

Certainly, to close this system of equations, we must supplement it with the algebraic equations

$$
\begin{aligned}
\boldsymbol{\sigma} &= \det(\mathbf{g}) \, \mathbf{g}^{-1} \cdot (\lambda \operatorname{tr}(\mathbf{e}) \mathbf{E} + 2\mu \mathbf{e}) \cdot \mathbf{g}^{-T}, \qquad \chi_\rho = \rho \, \mathbf{g}^{-1} \cdot \cdot \boldsymbol{\chi}_g, \\
\mathbf{e} &= \frac{1}{2} (\mathbf{g}^{-T} \cdot \mathbf{g}^{-1} - \mathbf{E}), \qquad \mathbf{J}_g = \mathbf{E} \, \mathbf{v} \cdot \mathbf{g}.
\end{aligned}
\tag{58}
$$

Now we give an account of the main features of our approach:
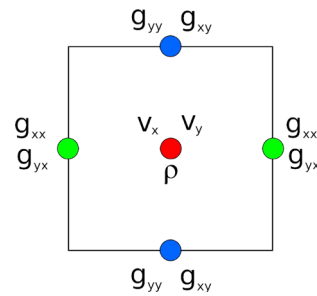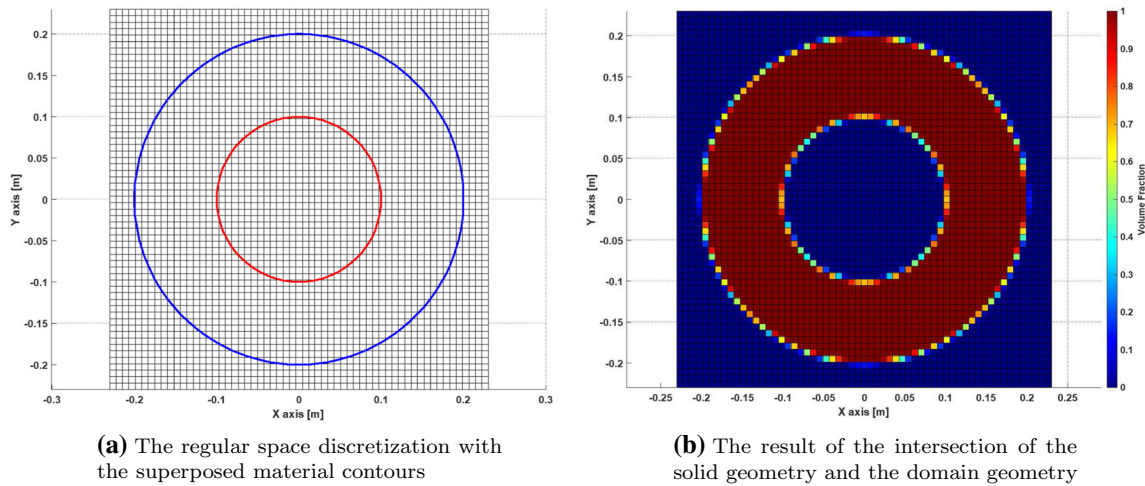
Fig. 1 The discretization scheme

– We use the components of strain measure **g** as the main variables. We include the equations relating the components of **g** to the components of velocity vector **v** into the system of the basic equations.
– We do not include the components of displacement vector **u** in the list of the basic variables and our system of the basic equations does not contain the equations for the components of vector **u**. If these quantities are needed, they can be calculated after the system of the basic equations is solved.
– We use the well-known staggered grid discretization scheme adapting it to our basic variables. Such scheme allows us to to work with highly irregular grids, such that the height and width of elementary cells differ by more than 100 times.
– We employ an explicit time-marching scheme. The fact that our system of the basic equations includes the equations for strains instead of the equations for displacements does not affect the choice of the time integration step.
– We apply the initial marker functions to define the initial density of the material and to construct the initial material interface. We employ the front tracking technique to define new positions of the material interface at each subsequent time step.
– We do not formulate any additional conditions at the boundary of the material if this boundary does not coincide with the boundary of the calculation domain. We take into account the Neumann boundary conditions by means of the corresponding body forces in the equations of motion. In the case of the kinematic boundary conditions, we use them instead of the equations of motion.

3.1 The staggered grid discretization scheme

We use *the staggered grid discretization scheme*, where different variables are assigned at different points of the control volume. This technique of the spatial discretization allows one to reduce computational errors and make the computational procedure more stable. This technique has a significant advantage over collocated grid discretization, where all variables are defined at the same points of the control volume. The staggered grid discretization is the well-known technique and it is often used in the finite volume method. But we suggest an original formulation of the problem, where the components of the strain measure play the role of the basic variables. Therefore we are forced to adapt this technique to the variables that we use. We assign the velocity projections v_x and v_y and the mass density ρ at the cell centers, the components of the strain measure g_{xx} and g_{yx} at the centers of the vertical sides, the components of the strain measure g_{yy} and g_{xy} at the centers of the horizontal sides. The discretization scheme is illustrated in Fig. 1.

3.2 The choice of the time step

Since we use the explicit time-marching scheme, we choose the time step based on the Courant–Friedrichs–Lewis number, which is defined as $\mathrm{CFL} = c\Delta t/\Delta x$, where c is the maximal signal propagation speed; Δt is the time step discretization; and Δx is the minimal spatial step in the calculation domain. It is known that $\mathrm{CFL} < 1$ guarantees stability for almost all explicit schemes. By numerical experiments, we found that $\mathrm{CFL} = 0.25$ ensures the convergence of our numerical scheme.

(a) The regular space discretization with the superposed material contours

(b) The result of the intersection of the solid geometry and the domain geometry

Fig. 2 An example of the marker function

3.3 Constructing of the initial marker function

We use *the marker function* to compute the average mechanical properties on the elementary cell, such as the initial mass density, Young's modulus and Poisson's ratio, and also to define the interface of the material for those cells which are partially filled with the material. The marker function is defined as the ratio of the volume of material in the given cell to the volume of the whole cell. It takes values between 0 and 1. Value 0 means that the material is absent in the cell. Value 1 means that the cell is completely filled with the material. All other values mean that the cell is partially filled. The procedure for constructing the initial marker function is as follows:

– to generate the domain geometry using Gmsh open source software and employing $Q9$ elements (the rectangle with 9 nodes);
– to generate the solid geometry using Gmsh open source software and employing $T3$ elements (the triangle with 3 nodes);
– export two geometries into MATLAB and set the data and connectivities;
– to perform a set of intersection boolean operations between the solid geometry and each elementary cell in order to define the initial marker function in all elementary cells of the computational domain.

In order to illustrate the procedure, we give an example, see Fig. 2. A regular volume with two contours, which represent the internal and external boundaries of the material is shown in Fig. 2a. The result that we obtain after performing the procedure is shown in Fig. 2b.

3.4 The front tracking technique

The front tracking technique is a numerical method that was first developed by Tryggvasson [37,45] to study multi-component flows. The main idea of the method is to track the material interface by interpolating the velocity vector at some points located at the material interface, e.g., point P in Fig. 3. As soon as the interface velocity $\mathbf{v}_p$ is determined, we can find the new position of the interface.

In order to calculate the velocity vector of point P located at the material interface we use the bilinear interpolation:

$$\mathbf{v}_p^{t+1} = \sum_{i=1}^{4} \omega_i \mathbf{v}_i^{t+1}, \tag{59}$$

where $\omega_i = A_i / \sum A_i$ are the interpolation weights, A_i are the areas shown in Fig. 3, and $\mathbf{v}_i$ are the known velocities calculated at the centers of the neighboring cells.

After velocities $\mathbf{v}_p^{t+1}$ are found, we can determine new positions of the corresponding points of the material interface as:

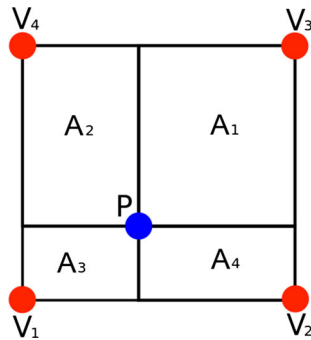$$\mathbf{r}_p^{t+1} = \mathbf{r}_p^t + \mathbf{v}_p^{t+1} \Delta t. \tag{60}$$

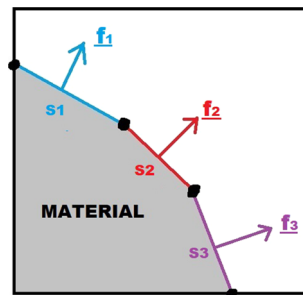**Fig. 3** The bilinear interpolation scheme

Fig. 4 The scheme for calculating the body force $\mathbf{f}_c$ equivalent to the Neumann boundary conditions

We note that, when analyzing the large strains, the pseudo-remeshing technique need to be applied at the material interface, because neighboring nodes can become distant from each other.

3.5 The Neumann boundary conditions

In the spatial description, the boundary conditions are formulated at the boundary of the computational domain. If the material boundary is inside the computational domain, then we have to set the Neumann boundary conditions by body force $\mathbf{f}_c$ in the linear momentum balance equation, see Eq. (9). The procedure for calculating $\mathbf{f}_c$ is as follows:

– to calculate length S_i for each segment of the material interface in the control volume, see Fig. 4;
– to calculate $\mathbf{f}_i = p_i S_i \mathbf{n}_i$, where p_i is the pressure on the segment and $\mathbf{n}_i$ is the normal vector to the segment, see Fig. 4;
– to calculate $\mathbf{f}_c = \sum \mathbf{f}_i / A_{vc}$, where A_{vc} is the area of the control volume (for 2D analysis).

4 Test problems

Below we consider five test problems illustrating the application of our method to model different mechanical processes in solids, such as the wave propagations, the flow of matter through the control volumes, and the dynamical processes in the matter caused by the source terms in the balance equations for the strains. For simplicity sake, we ignore the thermal effects and solve all the problems under the assumption of the plane strain, i.e., we suppose that all samples have the infinite length in the direction perpendicular to the plane x, y.

The first three problems are well known. We consider these problems in order to demonstrate that our method allows us to obtain quite adequate results when describing various mechanical processes. The first problem illustrates the propagation of initially plane waves, which are subsequently reflected from a circular hole. The second problem illustrates the generation and propagation of waves in the case of more complex geometry. The third problem shows the crack opening process and demonstrates the movement of matter through the elementary cells. The statements of the fourth and fifth problems are original, since they contain

the source terms in the equations for the strains. These problems differ from each other only by the source terms. The velocity of supplied matter $\mathbf{v}_*$ is assumed to be zero in both the problems. We consider the fourth and fifth in order to show that the presence of the source terms does not create any difficulties for the numerical procedure and leads to predictable results. Modeling of real physical processes by means of the source terms in the equations for strains is beyond the scope of our study.

In all the problems, we consider the samples occupying a part of the computational domain. Thus, we demonstrate the application of the font tracking technique for determining the location of the sample boundary at the current time and also the application of our technique of replacing the Neumann boundary conditions by the corresponding body forces. In all the problems, at the initial moment of time, the samples are at rest and their states are unstressed and unstrained. In all the problems, we use the same conditions at the boundary of the computational domain, namely, we assume that projections of the stress tensor on the normal to the boundary are equal to zero.

### 4.1 Problem 1: wave propagation in a solid sample with a circular hole

We consider a sample with the following parameters: the height of the sample is 0.1 m; its width is 0.2 m; the radius of the circular hole is 0.015 m; Young's modulus is 21.6 GPa; Poisson's ratio is 0.3; the mass density is 2500 kg/m^3. The wave processes in the sample are caused by the pressure acting on the vertical boundaries. If we used the material description, we would have to formulate the Neumann boundary conditions in the material description. But in the framework of the spatial description, we cannot formulate any additional equations at the boundary of the sample, since the boundary is inside the computational domain. That is why we replace the pressure at the vertical boundaries by the body forces evenly distributed over the elementary cells closest to the boundaries. These forces are directed along axis x at the left boundary and against axis x at the right boundary. The forces increase linearly with time, so that they equal to zero at the initial time point and reach the maximum value of 5 MPa at the final time point. The initial time point is zero, the final time point is 1 s. The horizontal boundaries of the sample are free. In the spatial description, these conditions are satisfied naturally. We use the space grid with 100 elements in the horizontal direction and 50 elements in the vertical direction. Sizes of the horizontal elements change from 2.08 mm (in the center of the computational domain) to 18.5 mm (near the left and right boundaries). Sizes of the vertical elements change from 1.41 mm (in the center of the computational domain) to 17.6 mm (near the top and bottom boundaries).

We now turn to the simulation results. The distributions of stresses σ_{xx} at four different moments of time are shown in Fig. 5. At the initial moment of time the stresses are absent, see Fig. 5a. The dots in Fig. 5a show the lagrangian discretization of the material interface. Employing these set of dots we determine the shape and location of the body at each time step. We observe two stress wave fronts in Fig. 5b. These waves start to propagate from the boundaries of the sample to its center. When the wave fronts reach the circular hole at the center of the sample, we observe the appearance of reflected waves, see Fig. 5c. Finally, we observe a stable and symmetric distribution of stresses, see Fig. 5d. In subsequent moments of time, the stresses increase linearly with increasing the external forces.

4.2 Problem 2: wave propagations in a thick walled cylinder

We consider a cylindrical sample with the inner radius equal to 0.08 m and the outer radius equal to 0.2 m. Young's modulus of the material is 10 GPa; Poisson's ratio is 0.3; the mass density is 2500 kg/m^3. The time-varying pressure acts on the inner surface of the cylinder, whereas the outer surface is fixed. In order to satisfy the boundary conditions at the outer surface, we replace the equations of motion in the cells closest to the outer surface by equations $v_x = 0$, $v_y = 0$. The conditions at the inner surface are, in fact, the Neumann boundary conditions. As in the previous problem, we model these boundary conditions by means of the body forces. In the case of the cylindrical sample, the body forces are evenly distributed over the elementary cells closest to the inner surface. These forces are directed along the radius of cylinder. The dependence of the body forces on time is exactly the same as in the previous problem. Thus, this problem is very similar to the previous one, but it allows us to demonstrate employing of our method in the case of the more complex geometry. We use the space grid with 51 elements in both the horizontal and the vertical directions. Sizes of elements change from 5.428 mm (in the center of the computational domain) to 25.0 mm (near the boundaries).

As in the previous problem, we show the distributions of stresses σ_{xx} at four different moments of time, see Fig. 6. The initial state with the zero stresses and the set of points, which discretize the interface of the

(a) Time $= 0$ s

(b) Time $= 7.5 \times 10^{-6}$ s

(c) Time $= 9.75 \times 10^{-5}$ s

(d) Time $= 8.99 \times 10^{-4}$ s
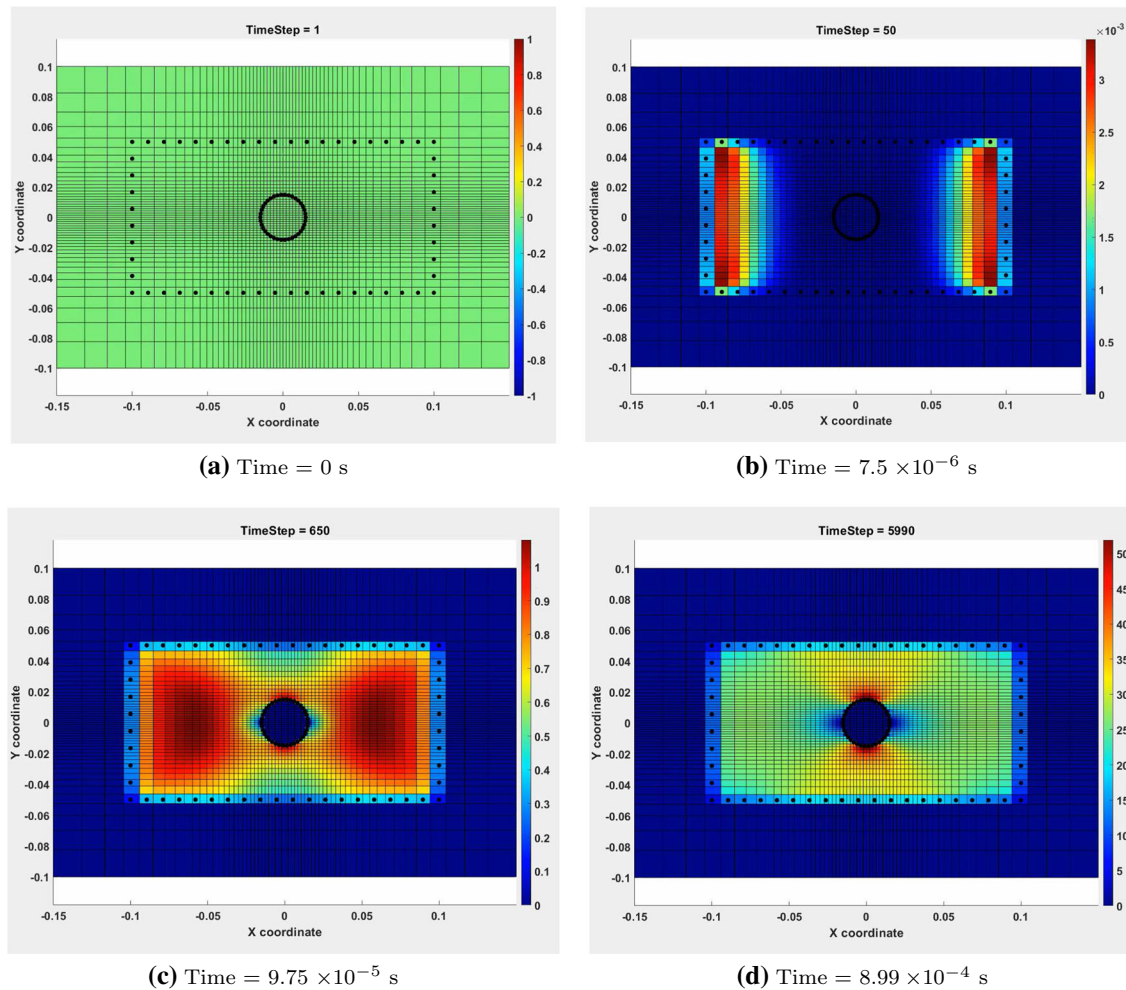
Fig. 5 Problem 1. Horizontal stress σ_{xx} in (Pa) at different time steps

material, is shown in Fig. 6a. One can observe four stress wave fronts in Fig. 6b. All of them propagate from the inner surface of the cylinder to its outer surface. Two waves are the compression waves. The other two waves are the extension waves. This is because the distribution of σ_{xx} is shown in Fig. 6, whereas the external load is radial. The distribution of stresses at the moment of time when the waves have already reached the outer surface of the cylinder is shown in Fig. 6c. The steady-state stress distribution can be found in Fig. 6d.

4.3 Problem 3: the crack opening process

We consider a sample with a crack located in its center. The sample height and width are equal to 0.35 m and 0.7 m, respectively. The crack height and width are equal to 0.1 m and 0.015 m, respectively. Young's modulus of the material is 1000 Pa; Poisson's ratio is 0.3; the mass density is 900 kg/m^3. The boundaries of the sample are assumed to be fixed. The crack opens due to the pressure acting on its vertical walls. We model the pressure by the body forces, evenly distributed over the elementary cells closest to the vertical walls. These forces are directed against axis x at the left wall and along axis x at the right wall. The dependence on time is the same as in the previous problems. We use the space grid with 120 elements in the horizontal direction and 60 elements in the vertical direction. Sizes of the horizontal elements change from 1.33 mm (in the center) to 92.4 mm (near the boundaries). Sizes of the vertical elements change from 4.57 mm (in the center) to 31.9 mm (near the boundaries).

(a) Time = 0 s

(b) Time = 5.75×10^{-5} s

(c) Time = 9.75×10^{-5} s

(d) Time = 1×10^{-3} s
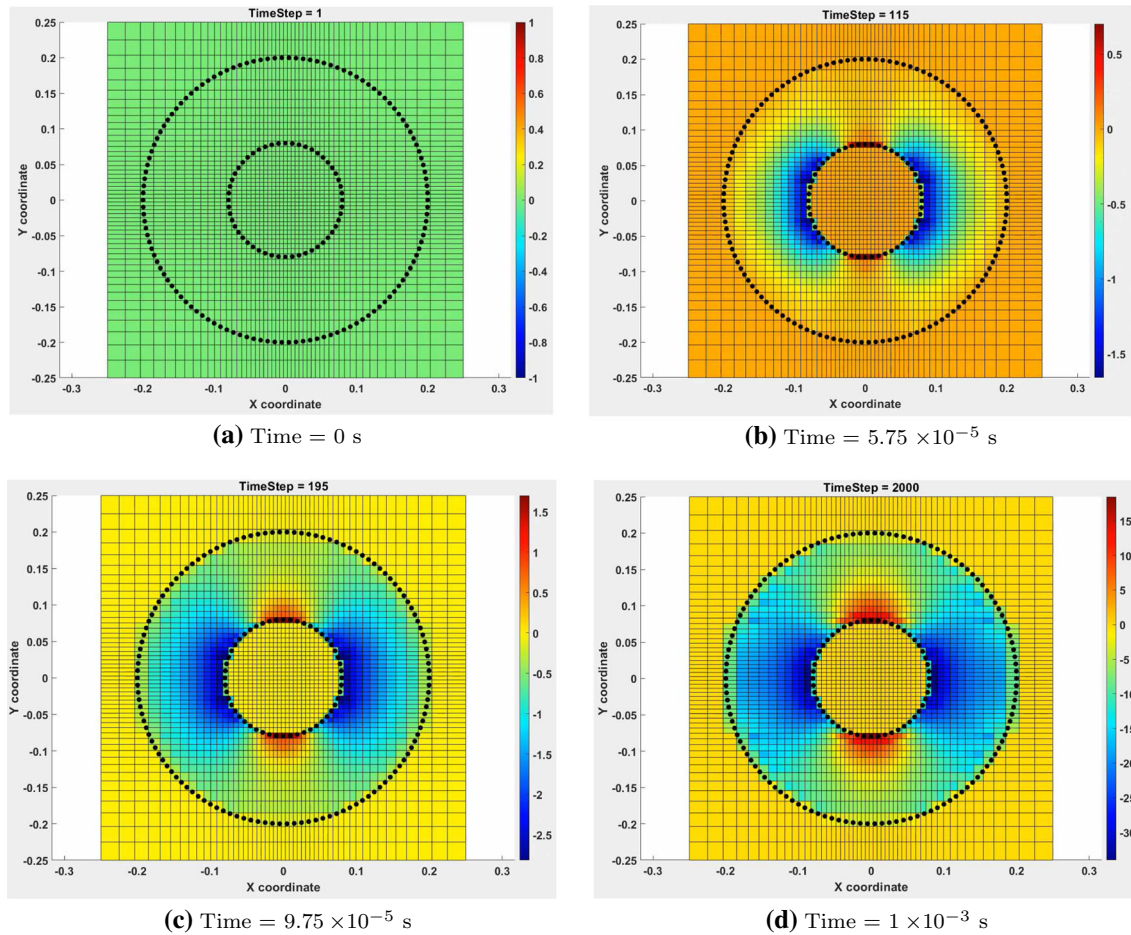
Fig. 6 Problem 2. Horizontal stress σ_{xx} in (Pa) at different time steps

The change of the density field near the crack seem to be the most interesting in this problem. It is shown in Fig. 7. The initial density field is in Fig. 7a, where the empty space is shown in blue and the crack walls are shown by a set of points discretizing the material interface. At the beginning of the process, when compression waves propagate from the crack and deformations of the crack walls are invisible so far, is shown in Fig. 7b. Later, the crack walls are displaced and noticeably deformed, see Fig. 7c. Some elementary cells previously filled with material become empty. This means that the material flows through the cells. The further development of the crack opening process, when even more empty cells appear, is shown in Fig. 7d.

4.4 Problem 4: strain sources distributed in a rectangular region

We now turn to the problem, where the external forces are absent and the stress–strain state of the material is caused only by the source term in one of the equations for strains. We consider a sample with the following geometrical and physical parameters: the height is 0.35 m ; the width is 0.7 m; Young's modulus is 21.6 GPa; Poisson's ratio is 0.3; the mass density is 2500 kg/m^3. The vertical and horizontal boundaries of the sample are fixed. We suppose that strain sources χ_{xx}^g are evenly distributed over the rectangular region $|x| \leq 2 \times 10^{-3}$ m, $|y| \leq 5 \times 10^{-2}$ m and do not depend on time. All other components of tensor χ_g are equal to zero. Component χ_{xx}^g equals -5×10^{-5} 1/s. We use the spatial grid as in the previous problem.
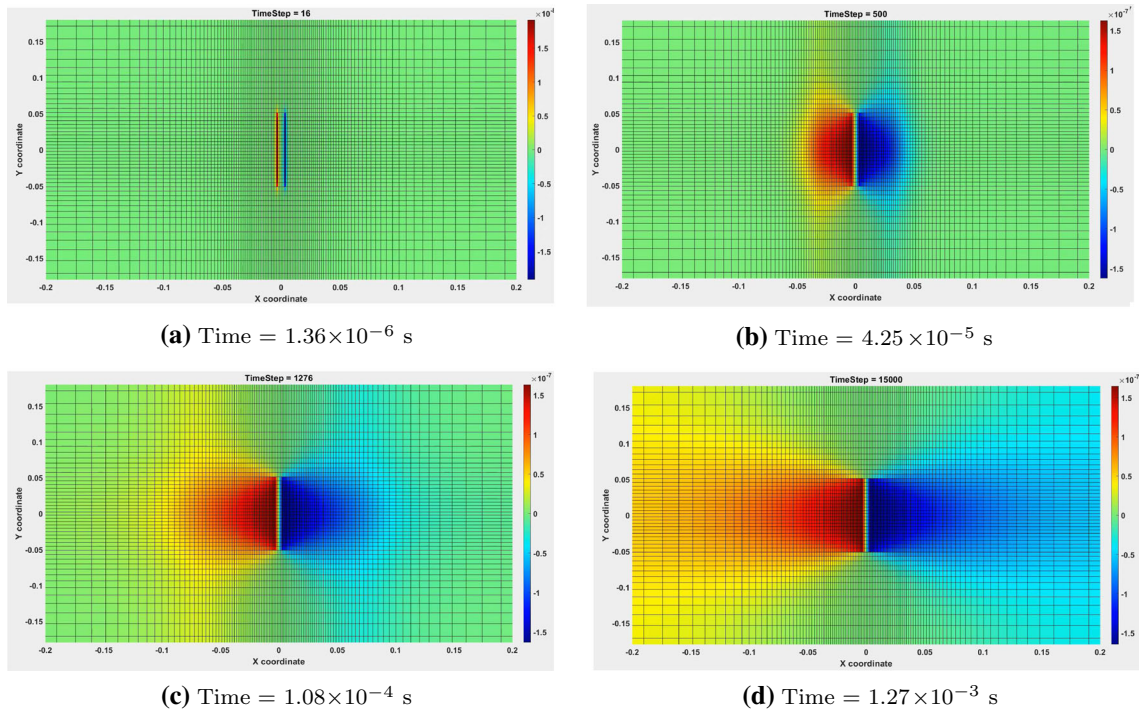
The density fields are shown in Fig. 8. At the initial moment of time, the density is evenly distributed over the whole region occupied by the material. In subsequent time points the density decreases significantly in the region where strain sources χ_{xx}^g are nonzero. Thus, some part of the material is removed from the central region of the sample, and as a result, this region is occupied by the material with a lower density. The horizontal
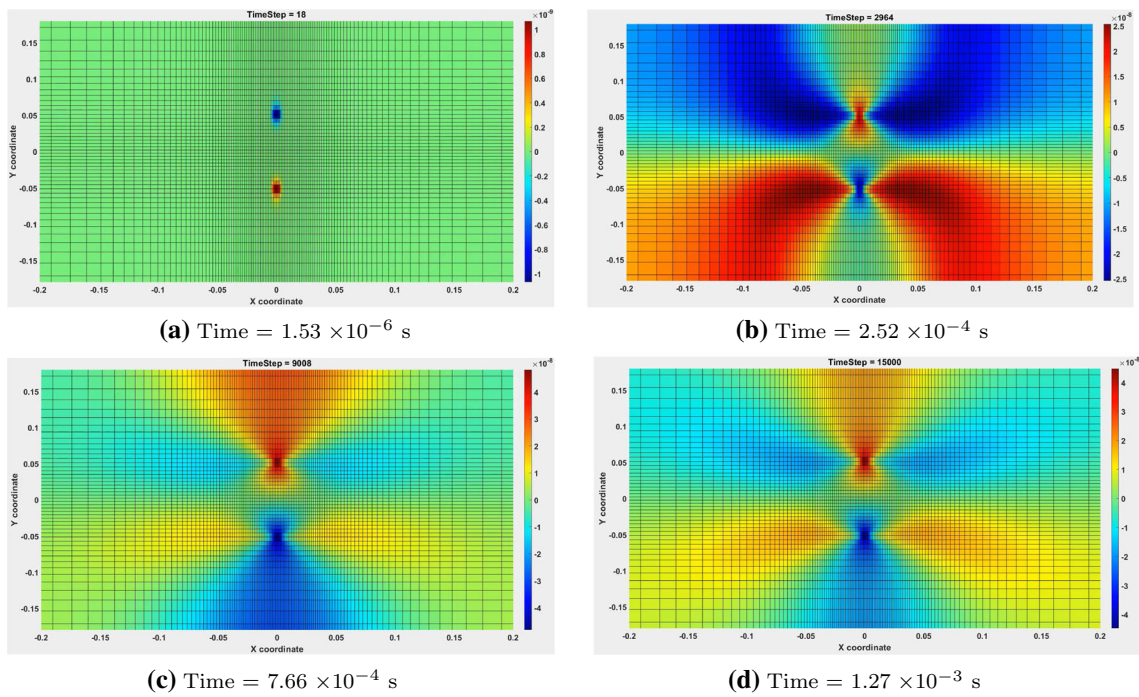
(a) Time = 0 s

(b) Time = 0.7625 s

(c) Time = 1.1225 s

(d) Time = 1.50 s
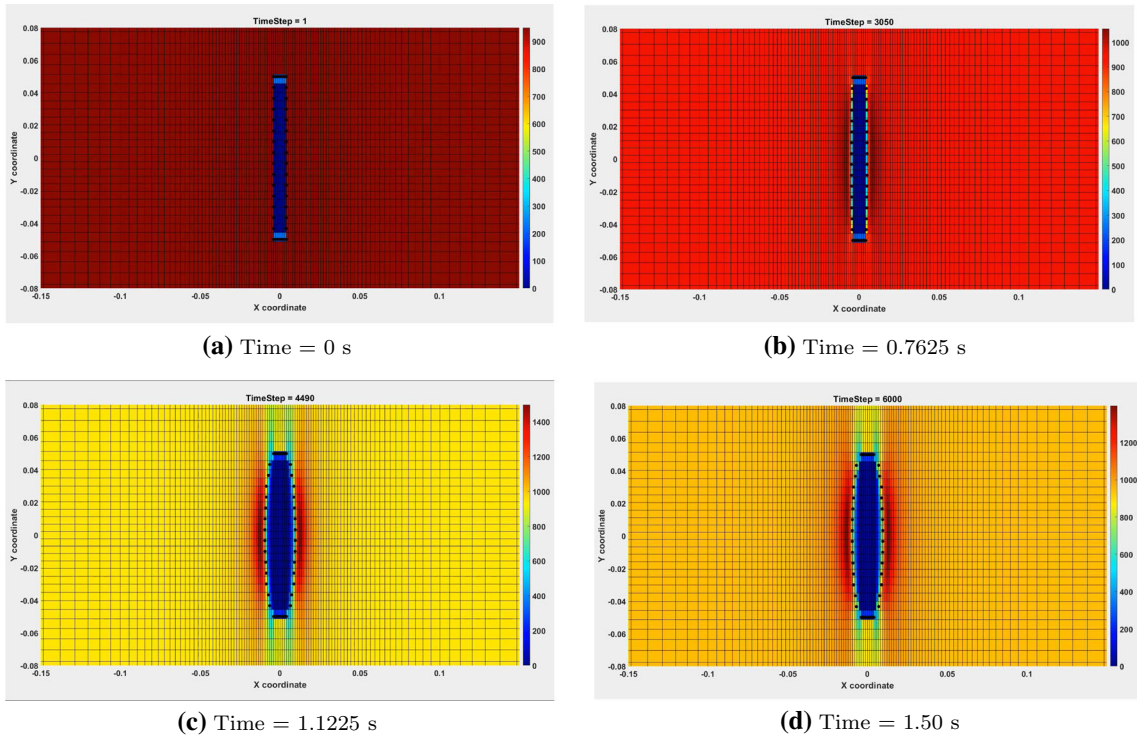
Fig. 7 Problem 3. Density field ρ in (kg/m^3) at different time steps (the figure is scaled to better fit the region of interest)

(a) Time = 0 s

(b) Time = 5.108×10^{-4} s

(c) Time = 1.019×10^{-3} s

(d) Time = 1.27×10^{-3} s
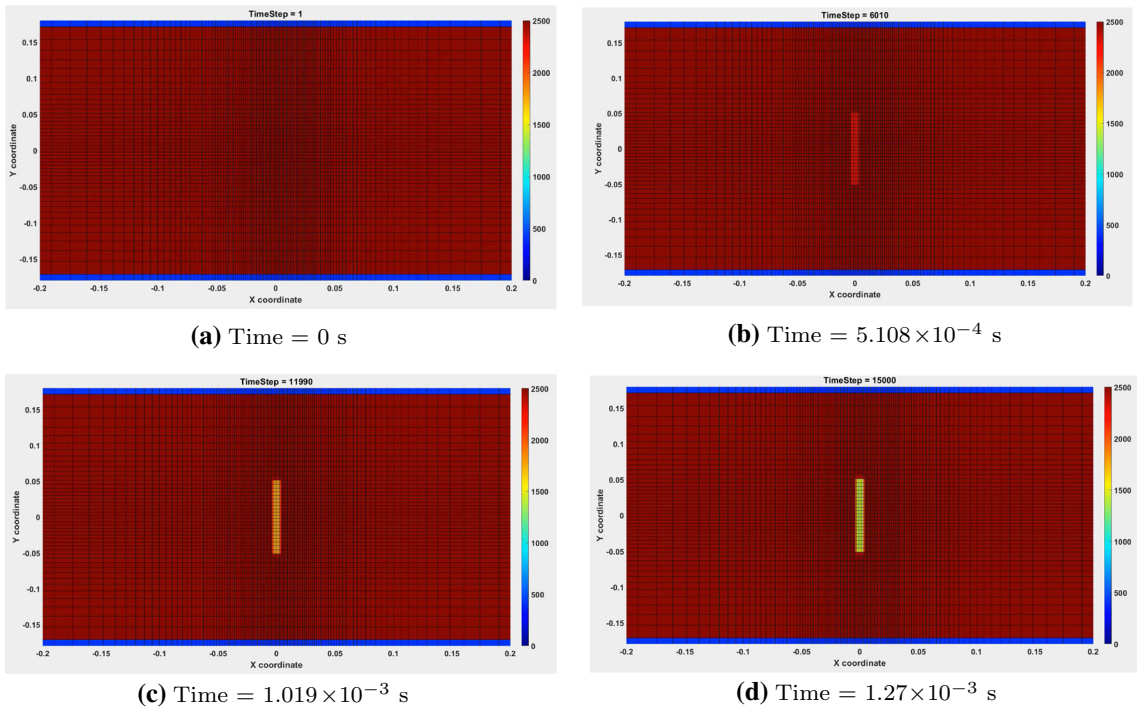
Fig. 8 Problem 4. Density field ρ in (kg/m^3) at different time steps (the figure is scaled to better fit the region of interest)

(a) Time $= 1.36 \times 10^{-6}$ s

(b) Time $= 4.25 \times 10^{-5}$ s

(c) Time $= 1.08 \times 10^{-4}$ s

(d) Time $= 1.27 \times 10^{-3}$ s

Fig. 9 Problem 4. Horizontal velocity field v_x in (m/s) at different time steps (the figure is scaled to better fit the region of interest)
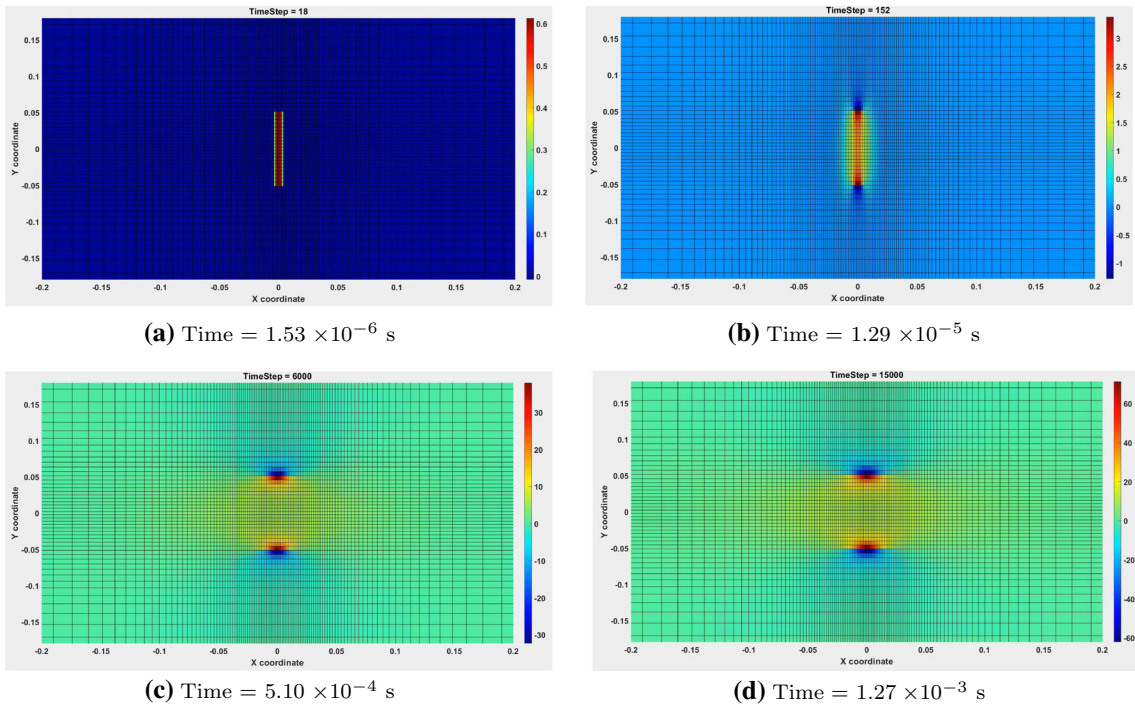

(a) Time $= 1.53 \times 10^{-6}$ s

(b) Time $= 2.52 \times 10^{-4}$ s

(c) Time $= 7.66 \times 10^{-4}$ s

(d) Time $= 1.27 \times 10^{-3}$ s

Fig. 10 Problem 4. Vertical velocity field v_y in (m/s) at different time steps (the figure is scaled to better fit the region of interest)

(a) Time = 1.53×10^{-6} s

(b) Time = 1.29×10^{-5} s

(c) Time = 5.10×10^{-4} s

(d) Time = 1.27×10^{-3} s

Fig. 11 Problem 4. Horizontal Stress σ_{xx} in (Pa) at different time steps (the figure is scaled to better fit the region of interest)
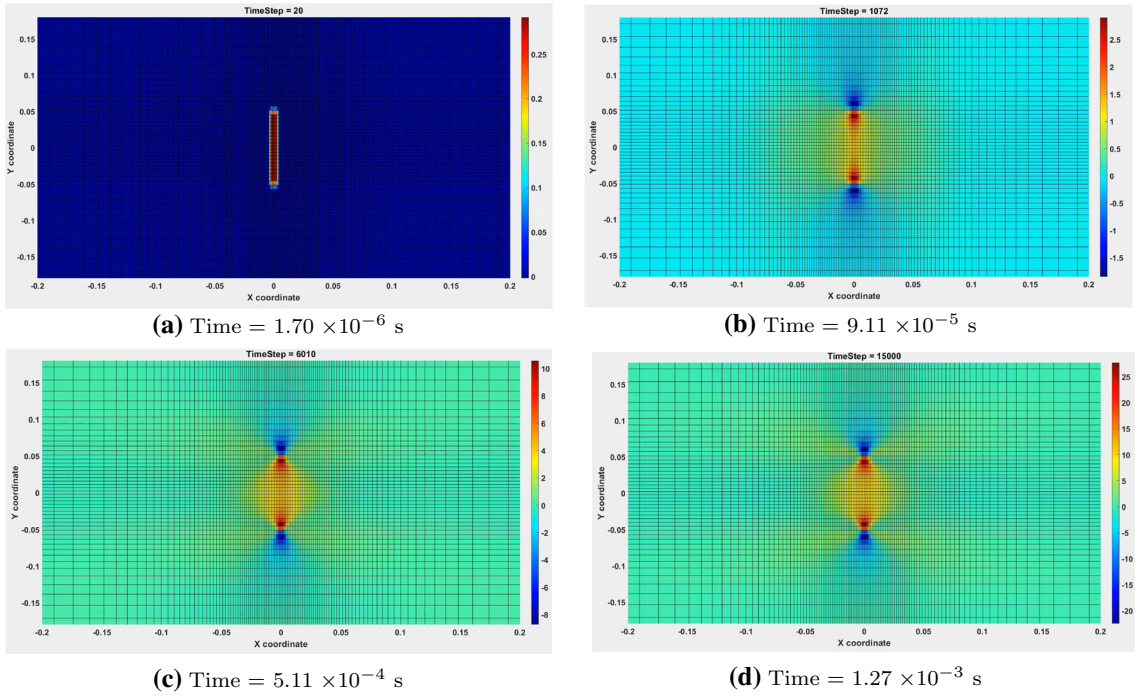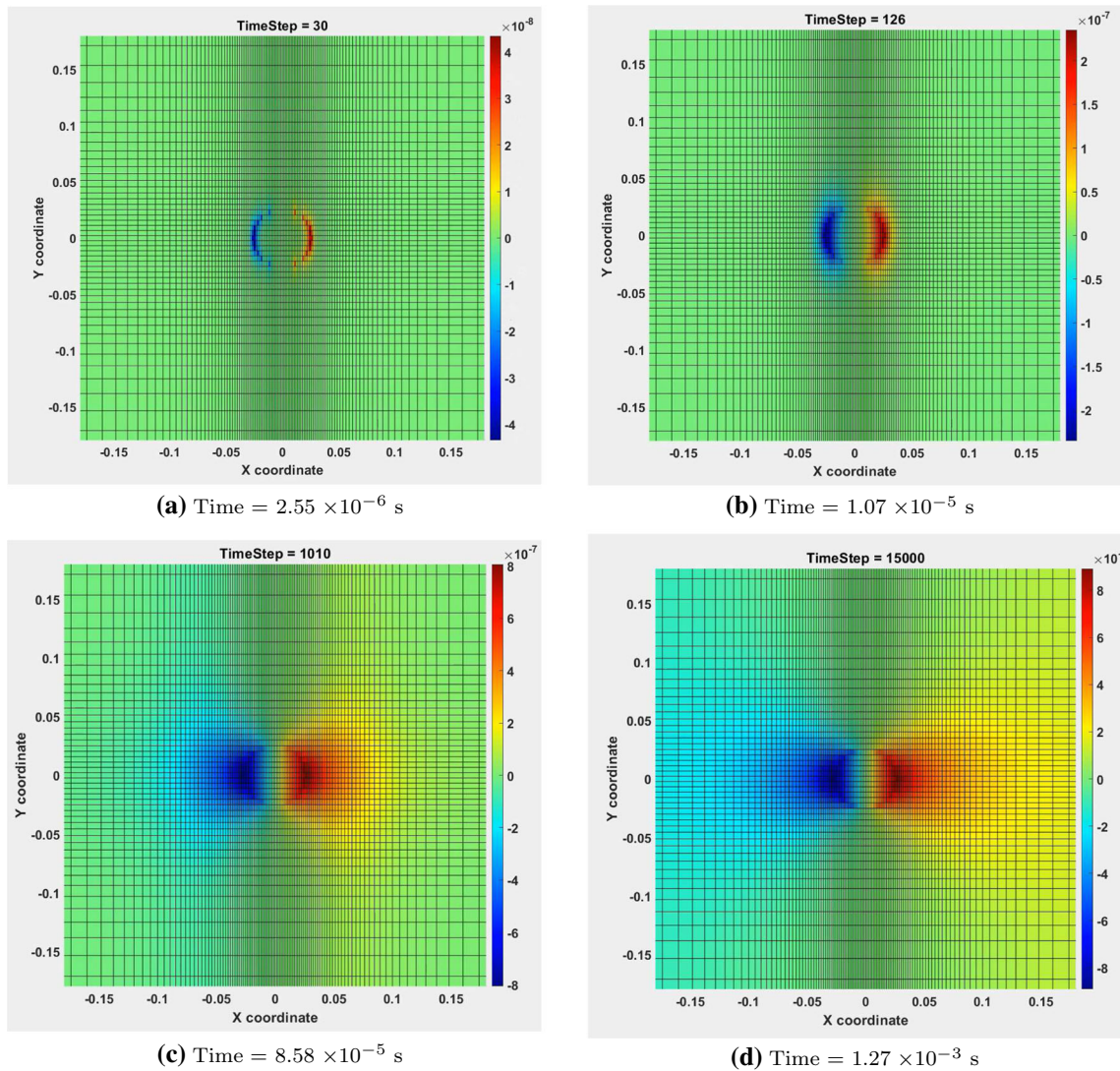

(a) Time = 1.70×10^{-6} s

(b) Time = 9.11×10^{-5} s

(c) Time = 5.11×10^{-4} s

(d) Time = 1.27×10^{-3} s

Fig. 12 Problem 4. Vertical Stress σ_{yy} in (Pa) at different time steps (the figure is scaled to better fit the region of interest)

(a) Time $= 2.55 \times 10^{-6}$ s

(b) Time $= 1.07 \times 10^{-5}$ s

(c) Time $= 8.58 \times 10^{-5}$ s

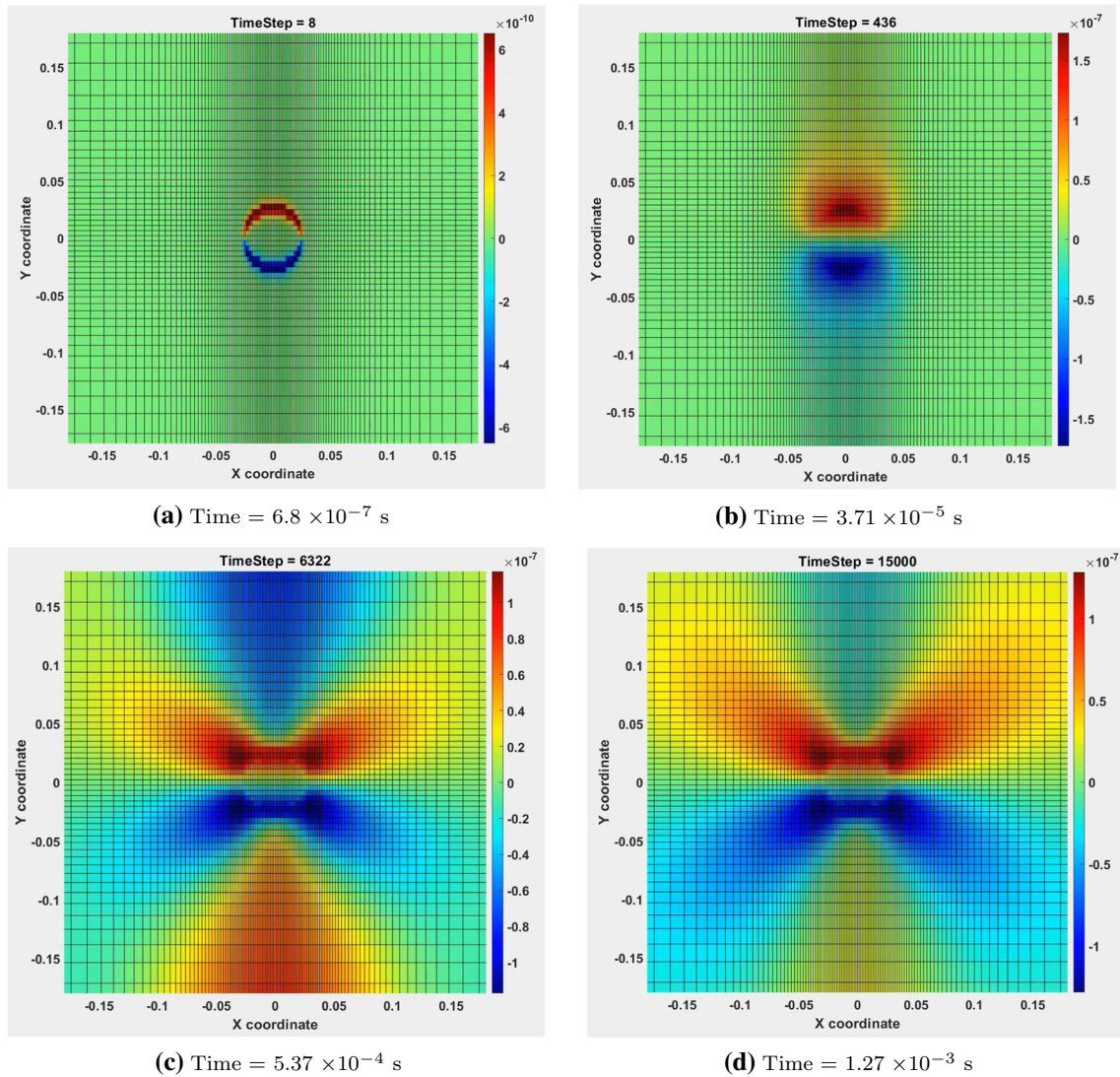**(d)** Time $= 1.27 \times 10^{-3}$ s

Fig. 13 Problem 5. Horizontal velocity field v_x in (m/s) at different time steps (the figure is scaled to better fit the region of interest)

velocity fields are shown in Fig. 9. It is seen, that the matter located on the left-hand side moves to the right, whereas the matter located on the right-hand side moves to the left. Thus, the matter flows towards the central region occupied by the material with a lower density. The vertical velocity fields are shown in Fig. 10. We see that at the beginning the material tends to flow to the center, but later some parts of the matter move towards the center, whereas some other parts flow from the center. This can be explained by the Poisson effect. The distributions of stresses σ_{xx} and σ_{yy} are shown in Figs. 11 and 12, respectively. At the beginning, we observe the even distributions of the stresses in the region of the strain sources and zero stresses in all other regions. Later, the stresses spread to larger regions and considerable concentrations of the stresses appear near the upper and lower boundaries of the region of the strain sources.

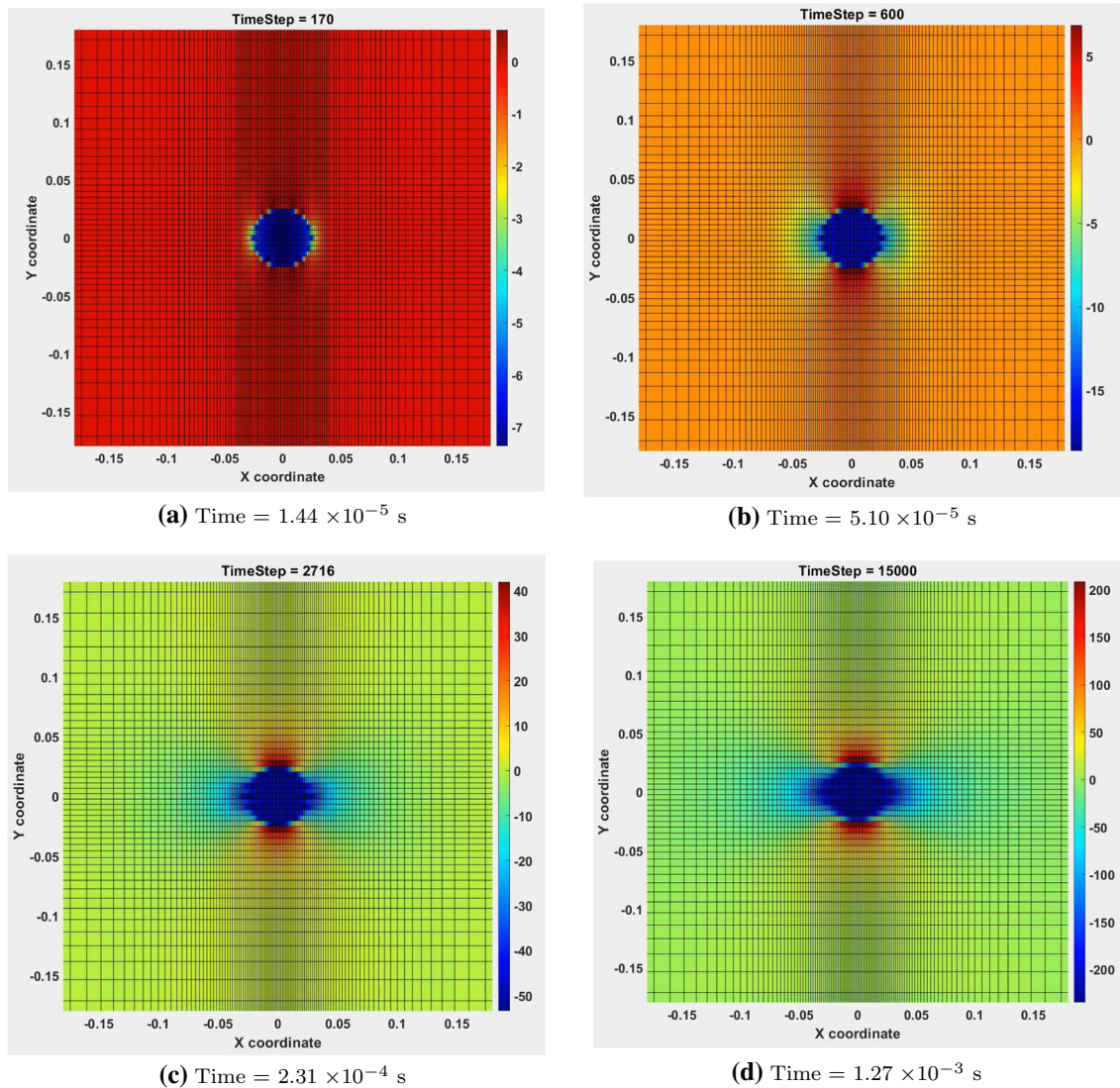4.5 Problem 5: strain sources distributed in a circular region

Now we consider the problem that differs from the previous one only by the strain sources. We assume that strain sources χ^g_{xx} and χ^g_{yy} are evenly distributed over the circular region $x^2 + y^2 \leq (2.5 \cdot 10^{-2})^2$ m^2 and do not depend on time. Component χ^g_{xx} equals to $5 \cdot 10^{-5}$ 1/s, component χ^g_{yy} equals to $5 \cdot 10^{-6}$ 1/s, the

Fig. 14 Problem 5. Vertical velocity field v_y in (m/s) at different time steps (the figure is scaled to better fit the region of interest)

other components of tensor $\boldsymbol{\chi}_g$ are zero. We emphasize that, in contrast to the previous problem, now we use where the source term was negative, in this problem the source terms are positive. This means that we add the material.

The horizontal velocity fields can be found in Fig. 13, where we can observe that the velocities are directed from the center and their values increase with time. The vertical velocity fields are in Fig. 14. It is easy to see that at the beginning the velocities are directed from the center, but later the vertical velocity fields become more complex. It is evident that the vertical velocity fields considerably differ from the horizontal ones. This is because the value of strain source χ_{yy}^g is much less than the value of strain source χ_{xx}^g. The distributions of stresses σ_{xx}, σ_{yy} and σ_{xy} can be found in Figs. 15, 16 and 17, respectively. One can observe that stresses σ_{xx} and σ_{yy} are negative in the region of the strain sources, whereas stresses σ_{xy} are zero in this region. The distributions of stresses σ_{xx} and σ_{yy} differ from each other. This is due to the considerable difference of the strain sources χ_{xx}^g and χ_{yy}^g. For the same reason, the concentrations of positive and negative stresses σ_{xy} appear near the boundary of the circle region. For the same reason, the concentrations of positive stresses σ_{xx} appear near the upper and lower parts of the circle region boundary, while these stresses remain negative near the left and right parts of the circle region boundary.

(a) Time $= 1.44 \times 10^{-5}$ s

(b) Time $= 5.10 \times 10^{-5}$ s

(c) Time $= 2.31 \times 10^{-4}$ s

(d) Time $= 1.27 \times 10^{-3}$ s

Fig. 15 Problem 5. Horizontal Stress σ_{xx} in (Pa) at different time steps (the figure is scaled to better fit the region of interest)

5 Conclusion

Now we emphasize three advantages of our approach. The first one is that we use only the instantaneous characteristics of the stress–strain state of solids as the main variables. Such an approach does not require the introduction of the reference configuration. This approach is typical for fluid and gas dynamics, but novel for the solid mechanics. We believe that our approach can be useful for describing dynamic processes in solids, when some parts of the material are deformed elastically, and plastic flow appears in other parts of the material. Our approach can also be useful for describing dynamic and quasi-static processes in the viscoelastic materials that behave like fluids, e.g., Maxwell's material. The second advantage of our approach is that we introduce the source term to the equation for the strain measure. Thus, we have expanded the concept of strains, taking them beyond the purely geometrical characteristics. This idea is novel. We believe that our definition of strains can be useful for modeling various processes in multi-component media containing solids. For example, one can use it to model chemical reactions which result in changes in mechanical states and mechanical properties of solids. We are convinced that our definition of strains can be applied not only to solving problems related to the supply of matter from an external source. It can be also applied to the description of phase transitions and structural changes that occur without a change in mass. The third advantage of our approach is that the

(a) Time = 6.97×10^{-6} s

(b) Time = 2.67×10^{-5} s

(c) Time = 3.80×10^{-4} s

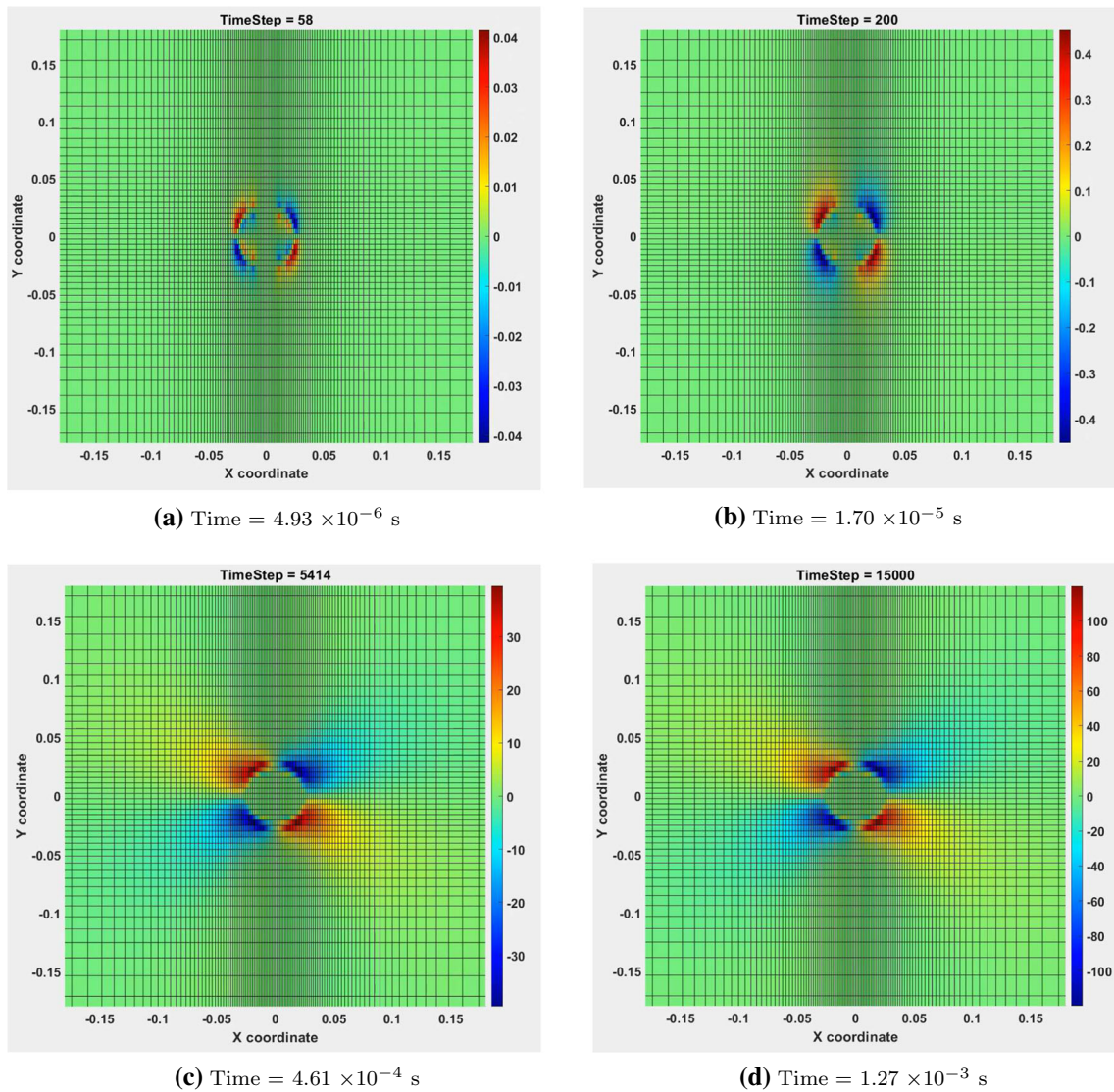**(d)** Time = 1.27×10^{-3} s
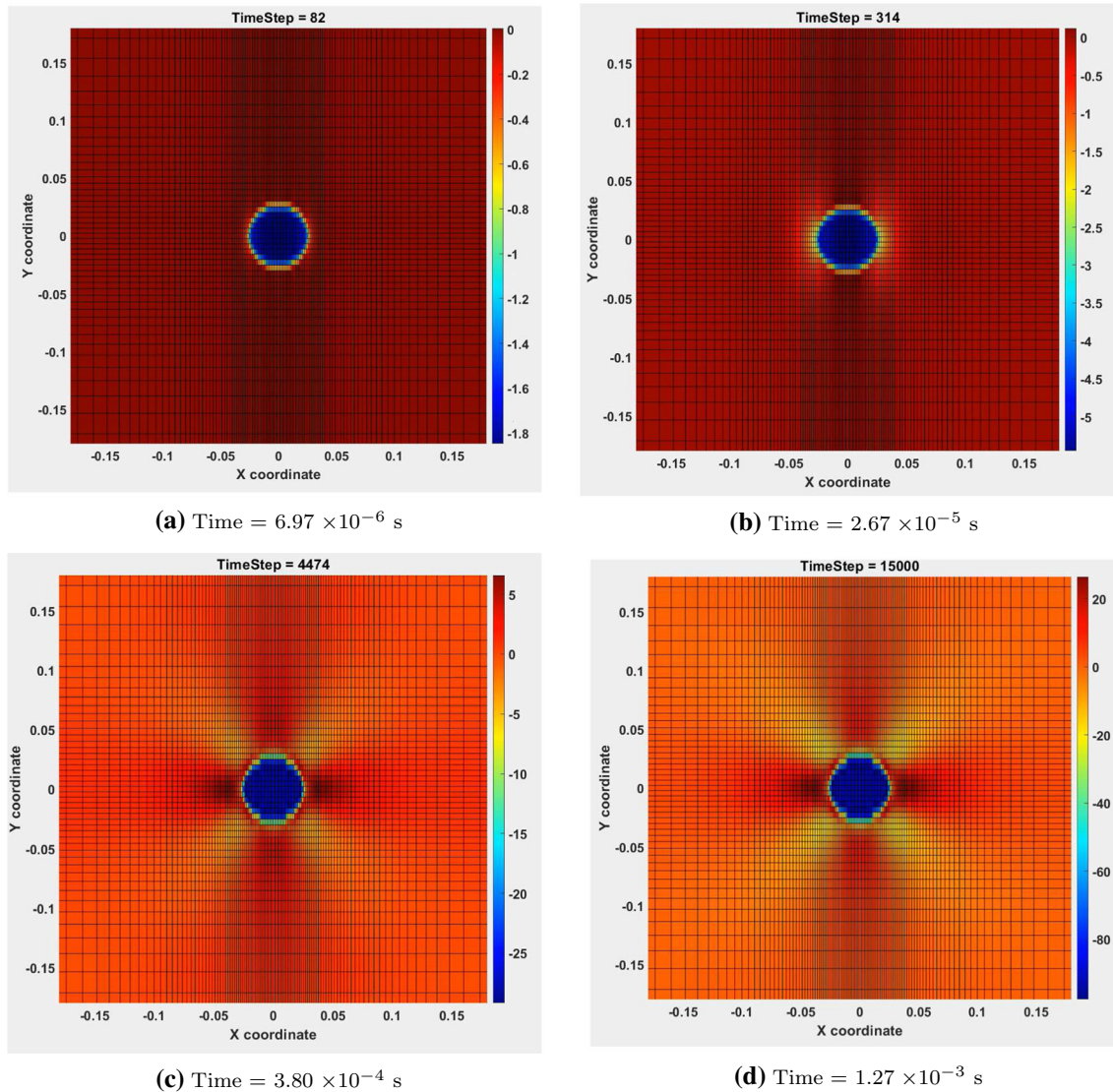
Fig. 16 Problem 5. Vertical Stress σ_{yy} in (Pa) at different time steps (the figure is scaled to better fit the region of interest)

presence of the source term in the equation for the strain measure provides additional opportunities to take into account the interaction of thermal and mechanical processes.

Within the framework of our approach, some questions remain open. They can be solved in different ways. For example, we can relate the mass density to the determinant of the strain measure, or we can consider it as an independent variable, see Sect. 2.9. Now it is unclear, which way is better. Also, we can use different definitions of the displacement vector, see Sect. 2.8. It is not yet clear, which definition is preferable. In addition, modeling different physical processes, we can imply different physical meanings of the source term in the equation for the strain measure. We can consider it to be a purely external factor or the result of some internal physical and chemical processes. Now it is difficult to say, which interpretation is more promising. All the above questions require further research.

(a) Time $= 4.93 \times 10^{-6}$ s

(b) Time $= 1.70 \times 10^{-5}$ s

(c) Time $= 4.61 \times 10^{-4}$ s

(d) Time $= 1.27 \times 10^{-3}$ s

Fig. 17 Problem 5. Stress component σ_{xy} in (Pa) at different time steps (the figure is scaled to better fit the region of interest)

References

1. Malvern, E.: Introduction to the Mechanics of a Continuous Medium. Prentice-Hall Inc, Englewood Cliffs (1969)
2. Truesdell, C.: A First Course in Rational Continuum Mechanics. The John Hopkins University, Maryland, Baltimore (1972)
3. Eringen, C.: Mechanics of Continua. Robert E. Krieger Publishing Company, Huntington (1980)
4. Batchelor, G.: An Introduction to Fluid Dynamics. Cambridge University Press, Cambridge (1970)
5. Loitsyansky, L.G.: Fluid Mechanics. Nauka, Moscow (1987).. (**In Russian**))
6. Daily, J., Harleman, D.: Fluid Dynamics. Addison-Wesley, Massachusetts (1966)
7. Arienti, M., Hung, P., Morano, E., Shepherd, J.E.: A level set approach to Eulerian–Lagrangian coupling. J. Comput. Phys. **185**, 213–251 (2003)
8. Donea, J., Giuliani, S., Halleux, J.P.: An arbitrary Lagrangian–Eulerian finite element method for transient dynamic fluid-structure interaction. Comput. Method. Appl. Mech. **33**, 689–723 (1982)

9. Hirt, C.W., Amsden, A.A., Cook, J.L.: An arbitraty Lagrangian–Eulerian computing method for all flow speeds. J. Comput. Phys. **14**, 227–253 (1974)
10. McGurn, M.T., Ruggirello, K.P., DesJardin, P.E.: An Eulerian–Lagrangian moving inmersed interface method for simulation burning solids. J. Comput. Phys. **241**, 364–387 (2013)
11. Surana, K.S., Blackwell, B., Powell, M., Reddy, J.N.: Mathematical models for fluid–solid interaction and their numerical solutions. J. Fluid. Struct. **50**, 184–216 (2014)
12. Brazgina, O.V., Ivanova, E.A., Vilchevskaya, E.N.: Saturated porous continua in the frame of hybrid description. Contin. Mech. Thermodyn. **28**(5), 1553–1581 (2016)
13. Pietraszkiewicz, W., Eremeyev, V.A.: On natural strain measures of the non-linear micropolar continuum. Int. J. Solids Struct. **46**(3–4), 774–787 (2009)
14. Chung, T.: Computational Fluid Dynamics. Cambridge University Press, Cambridge (2012)
15. Zienkiewicz, O.C., Taylor, R.L.: The Finite Element Method for Solid and Structural Analysis. ElSevier, Netherlands (2005)
16. Chandrupatla, T.R., Belegundu, A.D.: Introduction to Finite Elements in Engineering. Prentice Hall, United States (2002)
17. Wilmanski, K.: Thermomechanics of Continua. Springer, Berlin (1998)
18. Bowen, R.M.: Theory of Mixtures, Part I. Continuum Physics. III. Ed. A.C. Eringen. Academic Press, New York (1976)
19. Miller, G.H., Colella, P.: A conservative three-dimensional Eulerian method for coupled fluid-solid shock capturing. J. Comput. Phys. **183**(1), 26–82 (2002)
20. Benson, D.J., Okazawa, S.: Contact in a multimaterial Eulerian finite element fomulation. Comput. Methods Appl. Mech. Eng. **193**, 4277–4298 (2004)
21. Al-Athel, K.S., Gadala, M.S.: Eulerian volume of solid (VOS) approach in solid mechanics and metal forming. Comput. Methods Appl. Mech. Eng. **200**(25–28), 2145–2159 (2011)
22. Schoch, S., Nordin-Bates, K., Nikiforakis, N.: An Eulerian algorithm for coupled simulations of elastoplastic-solids and condensed-phase explosives. J. Comput. Phys. **252**, 163–194 (2013)
23. Ortega, A.L., Lombardini, M., Pullin, D.I., Meiron, D.I.: Numerical simulation of elastic–plastic solid mechanics using an Eulerian stretch tensor approach and HLLD Riemann solver. J. Comput. Phys. **257**, 414–441 (2014)
24. Ivanova, E.A., Matias, D.V., Stepanov, M.D.: Employment of Eulerian, Lagrangian, and Arbitrary Lagrangian–Eulerian decription for crack opening problem. Mater. Phys. Mech. **42**, 470–483 (2019)
25. Altenbach, H., Naumenko, K., Zhilin, P.A.: A micro-polar theory for binary media with application to phase-transitional flow of fiber suspensions. Contin. Mech. Thermodyn. **15**(6), 539–570 (2003)
26. Zhilin, P.A.: Advanced Problems in Mechanics, vol. 1. Institute for Problems in Mechanical Engineering, St. Petersburg (2006).. (**In Russian**))
27. Zhilin, P.A.: Advanced Problems in Mechanics, vol. 2. Institute for Problems in Mechanical Engineering, St. Petersburg (2006)
28. Zhilin, P.A.: Rational Continuum Mechanics. Polytechnic University Publishing House, St. Petersburg (2012).. (**In Russian**))
29. Ivanova, E.A., Vilchevskaya, E.N.: Micropolar continuum in spatial description. Contin. Mech. Thermodyn. **28**(6), 1759–1780 (2016)
30. Müller, W.H., Vilchevskaya, E.N., Weiss, W.: Micropolar theory with production of rotational inertia: a farewell to material description. Phys. Mesomech. **20**(3), 250–262 (2017)
31. Vilchevskaya, E.N.: On micropolar theory with inertia production. In: Altenbach, H., Öchsner, A. (eds.) State of the Art and Future Trends in Material Modeling, pp. 421–442. Springer, Berlin (2019)
32. Ivanova, E.A.: On a micropolar continuum approach to some problems of thermo- and electrodynamics. Acta Mech. **230**, 1685–1715 (2019)
33. Ivanova, E.A.: Derivation of theory of thermoviscoelasticity by means of two-component medium. Acta Mech. **215**, 261–286 (2010)
34. Ivanova, E.A.: Description of mechanism of thermal conduction and internal damping by means of two-component Cosserat continuum. Acta Mech. **225**, 757–795 (2014)
35. Ivanova, E.A.: A new model of a micropolar continuum and some electromagnetic analogies. Acta Mech. **226**, 697–721 (2015)
36. Ivanova, E.A.: Description of nonlinear thermal effects by means of a two-component Cosserat continuum. Acta Mech. **228**, 2299–2346 (2017)
37. Walter, J.: Eulerian Front Tracking for solid dynamics. Los Alamos National Research Laboratory, United States (1999)
38. Ivanova, E.A., Vilchevskaya, E.N., Müller, W.H.: Time derivatives in material and spatial description—What are the differences and why do they concern us? In: Naumenko, K., Aßmus, M. (eds.) Advanced Methods of Continuum Mechanics for Materials and Structures, pp. 3–28. Springer, Berlin (2016)
39. Ivanova, E.A., Vilchevskaya, E.N., Müller, W.H.: A study of objective time derivatives in material and spatial description. In: Altenbach, H., Goldstein, R., Murashkin, E. (eds.) Mechanics for Materials and Technologies. Advanced Structured Materials 46, pp. 195–229. Springer, Cham (2017)
40. Trangenstein, J.: Numerical Solution of Hyperbolic Partial Differential Ecuations, pp. 432–450. Cambridge University Press, Cambridge (2007)
41. Versteeg, H.K., Malalasakera, W.: An introduction to Computational Fluid Mechanics, pp. 129–225. Pearson Education, New York (2007)
42. Machado D.: Solucion numerica de las ecuaciones de Navier Stokes utilizando metodos tipo VOF, Universidad Simon Bolivar, Venezuela, pp. 30-45 (2019) (in spanish)
43. Kamrin, K., Rycroft, C., Nave, J.C.: Reference map technique for finite-strain elasticity and fluid–solid interaction. J. Mech. Phys. **60**, 1952–1969 (2012)
44. Kamrin, K., Mani, A., Jain, S.: A conservative and non dissipative Eulerian formulation for the simulation of soft solids in fluids. J. Comput. Phys. **1**, 261–289 (2019)
45. Tryggvasson, G., Prosperetti, A.: Computational Methods for multiphase flow, pp. 50–86. Cambridge University Press, Cambridge (2007)

46. Tepole, A.: Growing skin: a computational model for skin expansion in reconstructive surgery. J. Mech. Phys. Solids **59**, 2177–2190 (2011)
47. Brackbill, J.U., Kothe, D.B., Zemach, C.: A continuum method for modeling surface tension. J. Comput. Phys. **100**, 335–354 (1992)